國立臺灣大學生物資源暨農學院生物環境系統工程學系

博士論文

Department of Bioenvironmental Systems Engineering

College of Bio-resources and Agriculture

National Taiwan University

Doctoral Dissertation

同位素闡釋濁水溪沖積扇含砷地下水

氮化合物之來源及轉化

Isotopic evidence and simulation of nitrogen sources,

transformation, and transport in arsenic-contaminated groundwater

of Choushui River alluvial fan

翁宗男

Tsung-Nan Weng

指導教授：劉振宇 博士

Advisor: Chen-Wuing Liu, Ph.D

中華民國 108 年 1 月

January 2019

摘要

本研究區域濁水溪沖積扇南端之淺層地下水含有高濃度砷,歷年研究報告指出此區砷主要釋出機制為含砷之無晶型氧化鐵的還原溶解作用,另過去研究報告曾探討濁水溪沖積扇沿海區域之鹽化地下水中硫的氧化還原循環對砷移動性之影響,結果顯示高砷鹽化類地下水砷主要受硫歧化作用與含砷氫氧化鐵還原溶解影響,高砷非鹽化類則顯示有人為抽水行為改變地下水氧化還原條件,促使含砷硫化物再氧化,吸附於硫化物表面上的砷因而釋放至地下水中。除硫酸鹽類外,根據相關化學反應式,氮的氧化還原循環亦可能影響地下水中砷的傳輸與宿命,惟其在砷的生地化循環過程中所扮演的角色目前尚無人研究。

根據本研究結果,濁水溪沖積扇之扇頂區域之地下水含有高濃度硝酸鹽,扇尾區域則普遍存在高濃度砷及氨氮,透過 $\delta^{15}N_{NO3}$ 及 $\delta^{18}O_{NO3}$ 繪圖,可得扇頂地下水中硝酸鹽來源主要由含氮肥料、動物糞肥、及人類排泄物等所貢獻,扇央及扇尾地下水中硝酸鹽則主要來自含氮肥料及海洋中硝酸鹽,並發現自扇頂至扇尾有脫硝現象發生。氮循環系統方面,透過氮氧同位素化學反應方程式及其與硝酸鹽濃度之繪圖,可得扇頂地下水有顯著硝化作用,扇央地下水中硝酸鹽之植物同化為硝酸鹽削減之主要控制因子,惟脫硝現象並不顯著,而高濃度之砷、氨氮、鐵及 $\delta^{15}N_{NO3}$ 之削減隱含著 feammox 作用的發生;扇尾地下水有顯著脫硝作用發生,並且可能伴隨著植物同化、含氮物質礦化、硝酸鹽異化還原氨氮等作用,促成一個硝酸鹽削減及氨氮增加的地下環境。$\delta^{15}N_{NO3}$、$\delta^{18}O_{NO3}$ 與砷濃度繪圖以及相關化學反應方程式,指出扇央地下水之 feammox 作用及扇尾地下水的脫硝作用為導致含砷之鐵氫氧化物還原溶解,並且釋出吸附砷至地下水的主要反應促使過程。

爾後,利用 PHREEQC 模擬軟體進行前述研究成果之模擬,除藉由現地環境氧化還原狀態及實驗數據驗證模擬結果外,亦推估了未來反應終止之可能最終狀態,

I

以及可能傳輸情形，進一步瞭解濁水溪沖積扇地下水含氮化合物影響砷之生地化循環過程。由 PHREEQC 模擬結果顯示，硝化或 feammox 主要發生在扇頂及扇央，扇尾則無明顯此反應，而根據硝酸鹽從扇頂至扇尾的濃度空間分布，指出脫氮及硝酸鹽異化還原氨氮從上游至下游漸序發生。依現地溶氧及氧化還原電位數據分析，扇央及扇尾屬較還原狀態，可促使脫氮及硝酸鹽異化還原氨氮反應的發生。針對砷的價態轉換模擬，扇頂三價砷減少而五價砷增加，扇央及扇尾，由溶氧及氧化還原電位觀察結果，模擬砷由三價轉化為五價之狀況非常顯著。$\delta^{15}N$ 的差異模擬結果，在扇央及扇尾均顯示增加，符合現地採樣結果及理論依據，即脫氮反應發生時，$\delta^{15}N$ 將會增加。

一維傳輸結果，硝酸鹽同化作用發生在扇央，而氨氮硝化作用則發生在扇頂，但不同年份模擬結果均有不同程度之時間位移。五價砷濃度於扇央開始增加，乃因含砷之鐵氫氧化物還原溶解並使砷脫附所造成；三價砷濃度則在扇尾開始時增加，主要由五價砷的還原轉換及持續性的鐵氫氧化物還原溶解所導致。二價及三價鐵在扇央初期，因鐵氫氧化物還原溶解而使濃度增加，而三價鐵接著轉換為二價鐵。二價鐵為主的環境，除了與地下水還原態環境有關外，也可能與 feammox 反應而直接產生二價鐵有關。
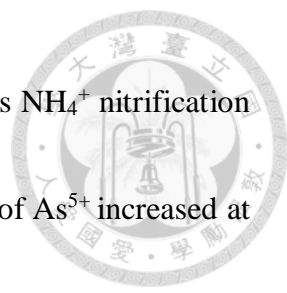
關鍵詞：地下水、砷、氮同位素、生地化循環

Abstract

In this study, on the basis of physicochemical characteristics of groundwater and the nitrogen and oxygen isotope composition of NO_3^-, it was inferred that the main sources of NO_3^- in the proximal fan of the Choushui River alluvial fan are likely to be ammonium fertilizers, manure, and septic waste; that in the mid-fan and the distal fan, the possible sources are nitrate fertilizers and marine nitrate. In the proximal fan, the oxidative state obviously promotes microbial nitrification. High DO concentrations and relatively low values of $\delta^{18}O_{NO3}$ in the deeper aquifer of the proximal fan may be attributed to unconfined granular nature and groundwater pumping by agricultural activities. In the mid-fan, NO_3^- assimilation is the dominant response to NO_3^- attenuation, and denitrification is insignificant; however, high concentrations of As, NH_4^+ and Fe and depletion of $\delta^{15}N_{NO3}$ imply the occurrence of feammox process. By contrast, denitrification evidently occurs in the distal fan, through assimilation, mineralization, and dissimilatory NO_3^- reduction to NH_4^+, resulting in depletion of NO_3^- and increase in NH_4^+ in groundwater. Feammox in the mid-fan and denitrification in the distal fan may be the main processes leading to the release of As from As-bearing Fe oxyhydroxides into groundwater.
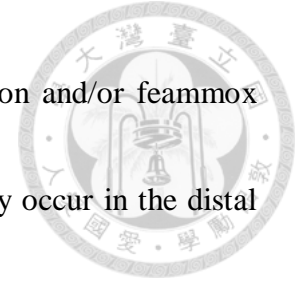
The simulation result of nitrification shows that the nitrification and/or feammox mostly occur in the proximal fan and mid-fan, whereas they slightly occur in the distal fan. The concentrations of NO_3^- and NH_4^+ in the proximal fan evidently support the occurrence of NH_4^+ nitrification. The spatial concentration distribution of NO_3^- from the proximal fan to the distal fan indicates the gradual occurrence of NO_3^- denitrification and/or DNRA from upstream to downstream of the Choushui River alluvial fan. The mid-fan and the distal fan were assessed on the basis of the local DO and ORP values to be in relatively more reductive conditions, driving the occurrence of denitrification and/or DNRA. In the proximal fan, As^{3+} decreased and As^{5+} increased, and this valence transformation of As species and As concentration difference seem comprehensible. In the mid-fan and the distal fan, the reductive state was observed base on the DO and ORP data of the groundwater, and the circumstance of reduction from As^{5+} to As^{3+} was obvious. The discrepancy of $\delta^{15}N$ in NO_3^- in groundwater was simulated on the basis of the influence of the reaction of NO_3^- denitrification. The values of $\delta^{15}N_{NO3}$ increased in the groundwater of the mid-fan and the distal fan; in theory, the denitrification increases $\delta^{15}N$ values of the residual NO_3^-.

The 1-D transport simulation result suggested that NO_3^- assimilation occur from the

IV

mid-fan of the Choushui River Alluvial Fan to the distal fan, whereas NH_4^+ nitrification

is observed at the beginning of the proximal fan. The concentration of As^{5+} increased at

the beginning of the mid-fan, which may be caused by the reductive dissolution of As-

bearing Fe oxyhydroxides and the desorption of adsorbed As. The concentration of As^{3+}

increased obviously at the beginning of the distal fan, which may be related to the

transformation of As^{5+} to As^{3+} in the reductive environment, and the continuous

desorption of As from Fe oxyhydroxides simultaneously. Both the concentrations of Fe^{3+}

and Fe^{2+} increased at the end of proximal, causing by the reductive dissolution of Fe

oxyhydroxides. The transformation of Fe^{3+} to Fe^{2+} occurred soon when the groundwater

reached the mid-fan. The increase in Fe^{2+} is not only related to the reductive environment,

but also attributed to the reaction of feammox, which Fe oxyhydroxides react with NH_4^+

and produce Fe^{2+} in the groundwater.

Keywords: Groundwater; Arsenic; Nitrogen isotope; Biogeochemical cycling

Contents

List of Tables

List of Figures

X

1. Introduction

Arsenic (As) is an ubiquitous trace metalloid found throughout the environment. The occurrence of As contamination in groundwater varies greatly due to the heterogeneous distribution of source materials and subsequent biogeochemical control on aqueous As mobility in aquifers. The major factor controlling the fate of As is the site-specific geochemical characteristics in different formation and the distribution of As is mostly associated with geological settings of the As-affected areas.

A nationwide contamination of As in groundwater has been observed in shallow tube wells in Bangladesh to depths of 15 to 30 m (Kinniburgh, 2001). Most wells of the shallow aquifers in coastal region were affected by As contamination (McArthur et al., 2001; Ravenscroft et al., 2001, 2005). Anawar et al. (2013) demonstrated that the As concentrations in groundwater of the Ganges delta within the depths of 30-40 m were strongly correlated with Holocene aquifer. Several release mechanisms of As have been postulated, yet the reduction of Fe oxyhydroxide is regarded as the most possible hypothesis (Eq. (1); Nickson et al., 1998; 2000). In Asia, high concentrations of naturally occurring As are often found in young alluvial and deltaic deposits with large amounts of fine grained detrital sediments together with fresh organic matter, except in mineralized

1

or mining areas (Plant et al., 2005; Mukherjee et al., 2006; Polizzotto et al., 2008). Besides, some studies also indicated the phenomenon that the in-situ distribution of As in groundwater accompanies with high NH_4^+-N concentration (Ravenscroft et al., 2005; Kurosawa et al., 2008).

$$8FeOOH\text{-}As_{(s)}+CH_3COOH+14H_2CO_3 \rightarrow 8Fe^{2+}_{(aq)}+As_{(d)}+16HCO_3^-_{(aq)}+12H_2O \qquad (1)$$

High concentrations of NH_4^+-N in groundwater, while not directly harmful to human health, are often a sign of the groundwater being affected by anthropogenic activities, such as spreading of fertilizers and manure or leaking sewage water (Vitòria et al., 2004; Hosono et al., 2011). Stüben et al. (2003) suggested that the presence of NH_4^+ reflects the reducing condition for release of As and Fe into groundwater. Kurosawa et al. (2008) reported that the NH_4^+ concentration is correlated positively with As concentration and negatively with oxidation reduction potential (ORP), thus the influence of N fertilizer application on As contamination is caused by reducing condition. High concentrations of NH_4^+ and As in shallow groundwater have also been simultaneously observed in the mid and distal fan of Choushui river alluvial fan (Fig. 1) (Agricultural Engineering Research Center, 2012). Therefore, NH_4^+ may be somehow correlated with As concentration in groundwater of this area, yet there has been few published reports discussing the coupled

2

correlation and interaction betweeen them.

The spatial distributions of NO_3^-, NH_4^+ contamination and high As concentrations occurred in Choushui river alluvial fan may not be effected by single occurrence. They may be governed by multiple geochemical processes, including either co-precipitation or adsorption of the reduction products, or both, that control the mobilization of As into the reductive groundwater.

However, most of previous studies only concern about NO_3^- contamination in groundwater by using N isotope as a single tracer. For example, stable N isotope has been used to identify sources of NO_3^- in groundwater (Peng et al., 2004; Peng and Fan 2005). Peng et al. (2012) reported that water mixing rather than isotopic fractionation processes such as denitrification or assimilation is the major process affecting the concentration and N isotope compositions of NO_3^- in trunk water. There has not yet been any published report discussing a correlation between As and N in groundwater by using multiple isotopes to identify the possible multiple redox processes of N regarding with As mobilization.
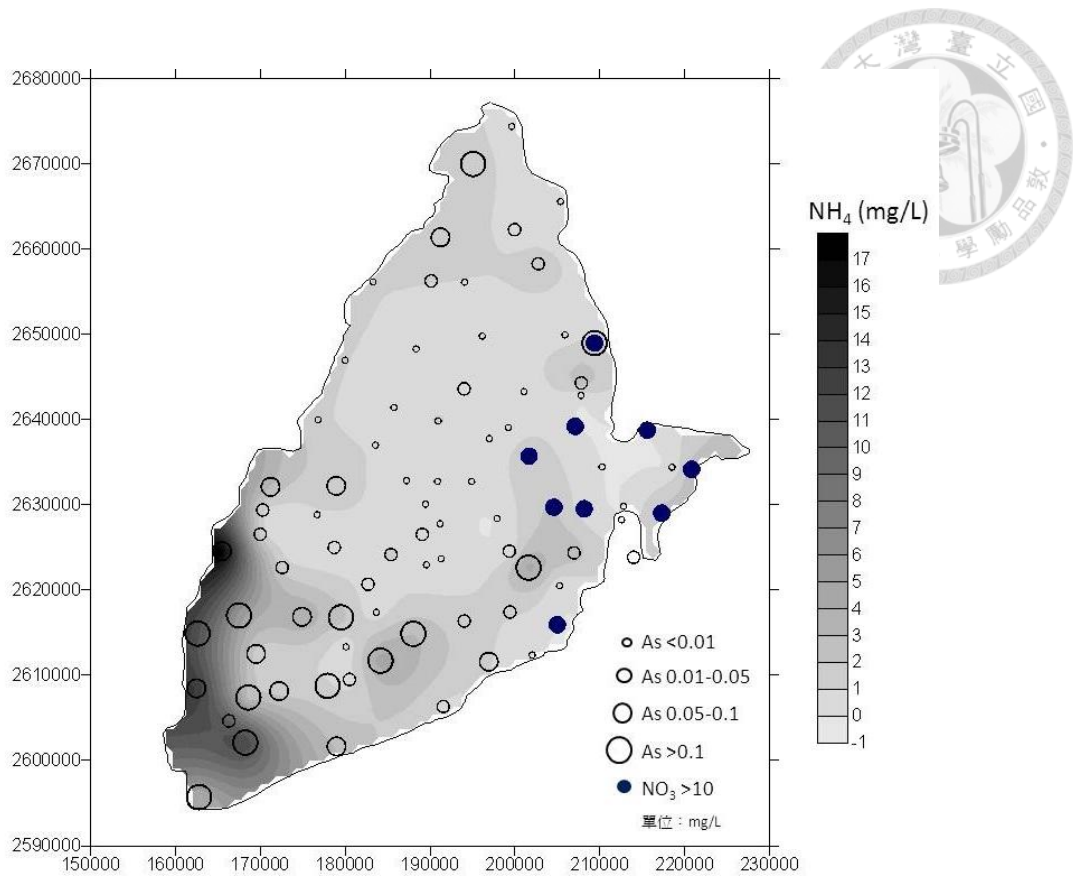
Fig. 1. Distribution of As, NH_4^+ and NO_3^- in groundwater of Choushui river alluvial fan.
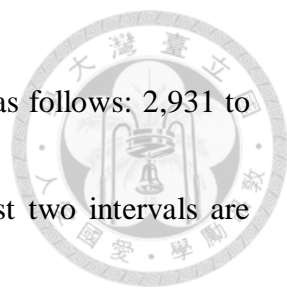
2. Literature reviews

2.1 Hydrogeochemical characteristics of As in Choushui River Alluvial Fan

Groundwater monitoring network in 10 groundwater divisions was established by Taiwan government in order to monitor the groundwater quality and level since 1999. Based on the groundwater monitoring network, Chianan Plain and Choushui river alluvial fan in southwestern Taiwan and Lanyang Plain in northeastern Taiwan are the main As-affected areas. In around 35 % of monitoring wells in Choushui river alluvial fan, As concentrations exceed the World Health Organization (WHO) guideline of 0.01 mg/L (Agricultural Engineering Research Center, 2012), and the highest As concentration is up to 0.96 mg/L (Agricultural Engineering Research Center, 2010).

According to the detailed analyses of sediment (Liu et al., 2006), considerable As contents enriched in the fine clay. Liu et al. (2006) showed that total As concentrations of core samples from the mid and distal fan were mostly higher than the average As content in crust (20 mg/kg). The highest As concentration of sediments in the shallow aquifer was in the depth of ~50 m, with the deposits of the Holocene transgression. The data from the accelerator mass spectrometry C^{14} dating of mollusk shells in the core samples of Choushui river alluvial fan (Central Geological Survey, 1999) suggested that the geologic

5

ages of the core samples in distal fan to mid fan could be grouped as follows: 2,931 to

5,364 yr ago, 7,090 to 9,230 yr ago, and >36,400 yr ago. The first two intervals are

associated with the formation of marine sequence 1, and the third is associated with the

formation of marine sequence 2. The As concentrations of the core samples in the second

interval exceeded those in the other two intervals, and the highest As concentration was

51.35 mg/kg (Liu et al., 2006). Based on the classification of the sedimentation sequences

(Huang, 1996), the second interval corresponded to the bottom of marine sequence 1,

which was mainly formed by clayey sediment. Additionally, the distribution of clay in

marine sequence 1 was more extensive than that in marine sequence 2, causing

considerable As accumulation. As concentrations in shallow strata of this area originated

primarily from aquitard formations of marine sequences, associating with the occurrence

of high As groundwater in shallow aquifer. Lu et al. (2010) also indicated well

correlations between As, S, and Fe concentrations of sediment by the results of XRF data.

The sequential extraction further showed that the major sinks of As were Fe minerals and

As-bearing sulfides under different redox conditions. Although the probable mechanism

of As released to groundwater was the dissolution of Fe minerals under reducing

conditions, the influence of SO_4^{2-}/S^{2-} reformation cycling on As mobility in aquifers did

6

not address.

2.2 N-budget system and applications of nitrogen/oxygen isotope in nitrate

Although NO_3^- is the most common N compound in oxygenated groundwater, NH_4^+ can be the dominant form because groundwater is in a strongly reductive state (Lindenbaum, 2012). The transformation processes among main N compounds (NO_3^-, NO_2^-, N_2O, NH_4^+, N_2) include the cycling processes of nitrification, denitrification, N fixation, assimilation, mineralization, anammox, and feammox (Fig. 2). Researchers often use the N isotope to identify the causes of depletion of and increase in each N compound and to distinguish between the sources of NO_3^- and NH_4^+ (Norrman et al., 2015; Scheiber et al., 2016; Otero et al., 2008; Hosono et al., 2011).

Due to its relatively stable characteristics, stable isotopes such as ^2H, ^{18}O, ^{34}S and ^{15}N have been useful in tracing the origins of water, contaminants and the source of dissolved constituents. Stable isotopes could be the fingerprints of the environment, regardless of temporal and geographic scales. For more than a decade, researchers in Taiwan have demonstrated considerable cases in evaluating the source of contaminants in groundwater. With information from local spatial distribution, researchers can provide strong and conclusive evidence about the source of contaminants, which is immediate

concern of the affected populace. As of, stable isotopes have been utilized to understand

the biogeochemical processes in groundwater systems as well (Kendall, 1998; Cook and

Herczeg, 2000; Kao et al., 2011).
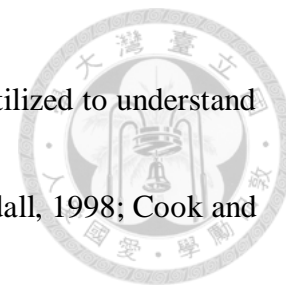
Many investigators have successfully applied several isotopes in groundwater

environment studies, including δD and $\delta^{18}O$ in H_2O, $\delta^{34}S$ and $\delta^{18}O$ in SO_4^{2-}, $\delta^{15}N$ and

$\delta^{18}O$ in NO_3^-. Briefly, δD and $\delta^{18}O$ have commonly been used to understand the origin

and mixing of H_2O in groundwater (Clark and Fritz, 1997; IAEA 1983). In Taiwan, the

stable isotopes δD and $\delta^{18}O$ are regarded as applicable tracers for investigating hydrologic

relations between different water bodies (Liu 1984; Wang and Peng 2001; Peng et al.,

2007). $\delta^{34}S_{SO4}$ and $\delta^{18}O_{SO4}$ have been useful in determining the sulfur cycling that occurs

in the coastal aquifer. The origin of SO_4^{2-} in groundwater is various, which may be derived

naturally during dissolution of gypsum or oxidation of S^{2-}. $\delta^{34}S_{SO4}$ and $\delta^{18}O_{SO4}$ have been

used as tracers of (1) in different natural sources of SO_4^{2-} (modern seawater, dissolution

of sulfate minerals, and soil sulfates) (Clark and Fritz, 1997; Krouse and Mauer, 2000);

(2) man-made SO_4^{2-} (sewage, agrochemicals, detergents and SO_4^{2-} of industrial origin)

(Torssander et al., 2006; Brenot et al., 2007; Otero et al., 2008); (3) S redox processes

(oxidation of S^{2-} and reduction of SO_4^{2-}) (Seiler et al., 2011; Kao et al., 2011). In addition,

many studies have been carried out using $\delta^{15}N_{NO3}$ and $\delta^{18}O_{NO3}$ in order to discriminate

between organic (e.g., human or animal manure) and inorganic (e.g., chemical fertilizers)

N contaminants in waters (Robinson and Bottrell, 1997; Otero et al., 2008; Hosono et al.,

2011).

Tracing of NO_3^- and SO_4^{2-} sources/sinks by N and S isotope compositions,

respectively, is depending on kinetic and thermodynamic fractionation processes. The

NO_3^- contamination in shallow groundwater may suffer by the combined impact of

fertilizer and septic tank effluent. The jointed data of ^{15}N and ^{18}O provide an effective

tool to distinguish between NO_3^- of different origin and to evaluate the N-budget of a soil-

water system (Fig. 3). The organic N, which is originated from manure or fertilizers, can

be transformed back to NH_4^+ for recycling in the N-budget system, and that the

commercial urea fertilizers (NH_2CONH_2) decompose in groundwater to NH_4^+ may also

be subsequently oxidized by nitrification to NO_3^- (Fig. 2; Eq. (2)).

In proximal fan of Choushui river alluvial fan, NO_3^- is the most stable species in

oxidizing condition in groundwater, and the various sources of NO_3^- can be distinguished

by analyzing ^{15}N and ^{18}O. Next, a variable biological reaction requires anoxic conditions

and accessible organic substrates such as dissolved organic carbon (DOC) (Eq. (3)).

9
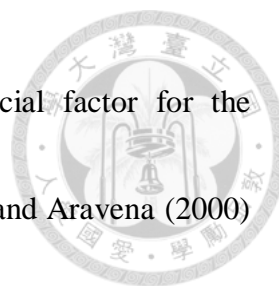
These principal N-transforming reactions are regarded as a crucial factor for the distribution of isotopes in NO_3^- and NH_4^+ in groundwater. Kendall and Aravena (2000) reported that the negative correlation of $\delta^{15}N_{NO3}$ versus NO_3^- concentration showed that the residual NO_3^- was enriched in ^{15}N exponentially as NO_3^- concentration decreased, which might be caused by denitrification process. The denitrification of a NO_3^- fertilizer with an original $\delta^{15}N_{NO3}$ value of +0 ‰ can yield residual $\delta^{15}N_{NO3}$ value of +15 to +30 ‰. However, it may be an obstacle in differentiating N sources, since the range is similar with that being expected from manure or septic waste (Clark and Fritz, 1997).

The NO_3^- contamination of shallow groundwater may result from the combined impact of fertilizer application and septic tank effluent leakage. The combination of $\delta^{15}N_{NO3}$ and $\delta^{18}O_{NO3}$ data can be effectively used for distinguishing between NO_3^- from different origins and for evaluating the N-budget of a soil-water system (Fig. 3).

Nitrification $\quad\quad\quad\quad NH_4^+ + 2O_2 \rightarrow NO_3^- + 2H^+ + H_2O$ $\quad\quad\quad\quad\quad\quad\quad\quad$ (2)

Denitrification $\quad\quad\quad NO_3^- + 5/4CH_2O \rightarrow 1/2N_2 + 5/4HCO_3^- + 1/4H^+ + 1/2H_2O$ $\quad\quad\quad$ (3)
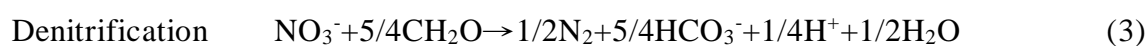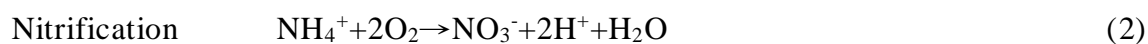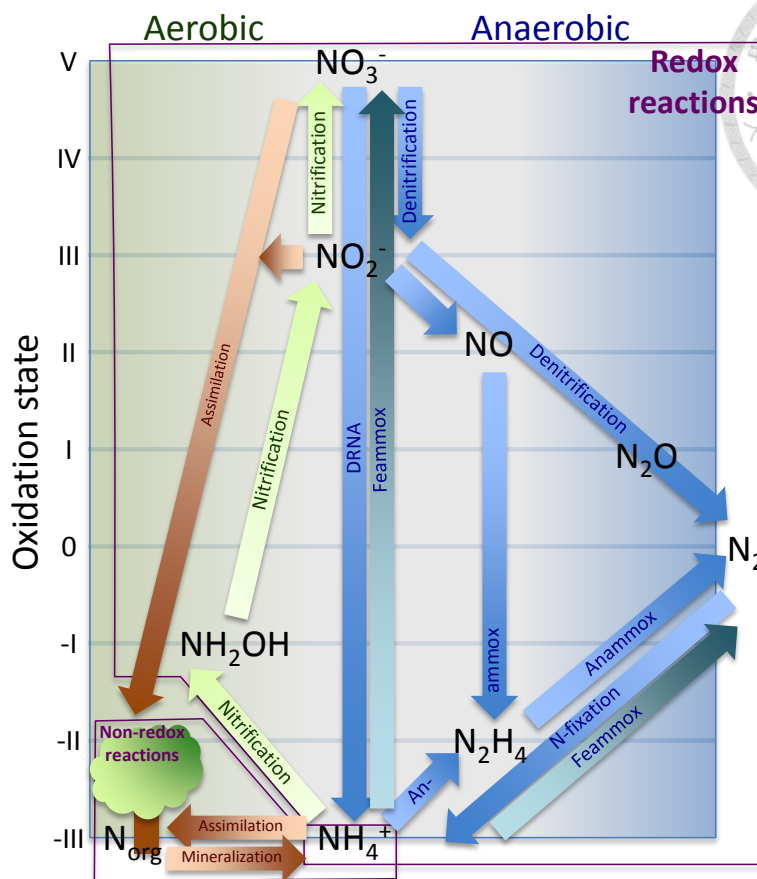
Fig. 2. Schematic of major N transformation pathways (modified from Canfield, 2010).
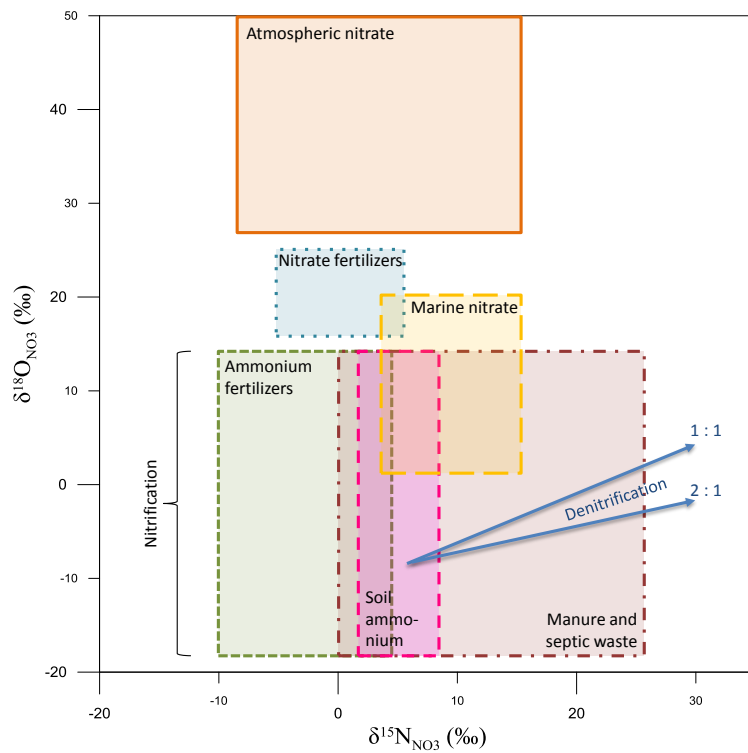
Fig. 3. Typical ranges of $\delta^{15}N_{NO3}$ and $\delta^{18}O_{NO3}$ values for various nitrate sources (modified from Kendall et al., 2007).

The purpose of the study is to identify of the possible multiple redox processes of N associated with As mobilization in groundwater. As we know, a few number of researches focused on the impact of N cycling on As migration. It has been reported that NO_3^- limited the reduction of iron oxides by consuming available electron donors, and consequently the release of As (Pauwels et al., 2000). Previous N isotope study showed that denitrification occurred in the aquifer (Li et al., 2010), yet the influence of denitrification on As mobilization remained to be understood. The negative linear relationship between NO_3^- and SO_4^{2-} during denitrification processes is governed by Eq. (4). In this process, the Rayleigh function can be applied to both ^{15}N and ^{18}O to determine the enrichment factors that dominate in groundwater. The oxidation of As-bearing pyrite results in subsequent As release, which can be identified by the correlation between $\delta^{34}S_{SO_4}$ and $\delta^{18}O_{SO_4}$ (Van Stempvoort and Krouse, 1994). The adsorption of As by newly precipitated hydrous ferric oxides may be occurred by Eq. (4), then reductive dissolution of As-$Fe(OH)_3$ may result in enrichment of As in groundwater of reducing conditions. However under typical aquifer conditions, iron (and sometimes manganese) sulfide (pyrite) is typically expected to be the electron donor (Korom, 1992; Ottley et al., 1997) (Eq. (5))

$$FeS_2 + 6NO_3^- + 4H_2O \rightarrow 2Fe(OH)_3 + 4SO_4^{2-} + 3N_2 + 2H^+ \qquad (4)$$

12

$$5FeS_2 +14NO_3^- +4H^+ \rightarrow N_2 + 10SO_4^{2-} + 5Fe^{2+} + 2H_2O \qquad (5)$$

$$0.5N_2 + 5FeOOH + 9H^+ \leftrightarrow NO_3^- + 5Fe^{2+} + 7H_2O \qquad (6)$$
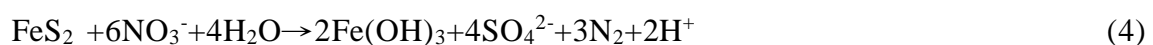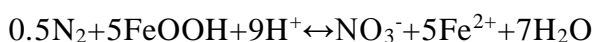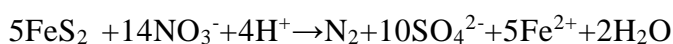
The reaction (Eq. (5)) is favorable in soils as adsorption of dissolved Fe^{2+} and NH_4^+ onto sediment particles, and the situation is described as a reversible, linear equilibrium reaction. Molecular oxygen was indirectly incorporated into the SO_4^{2-} via the sequestration by nitrification, however high salinity might inhibit denitrification (Rivett et al., 2008). Geochemical studies of S and N isotopes found that pyrite oxidation accounted for approximately 70% of the SO_4^{2-} present in the zone of denitrification (Zhang et al., 2014). Isotopic analysis suggested that denitrification might be fueled by Eq. (6). As NO_3^- was consumed, more goethite might dissolve, accompanying by the release of absorbed As. Hence, N isotope analysis can elucidate the presence of denitrification in groundwater; it may also be an important influencer of As mobilization. With the aid of multiple isotopes of H, O, S, and H, together with hydrogeochemical investigation, the biogeochemical processes occurring in groundwater system of Choushui river alluvial fan can be elucidated, and the geochemical behavior of As affected by the biologically uptakes of essential nutrients elements for metabolisms should be explained as well.

The results of isotopic compositions (δD and $\delta^{18}O_{H2O}$, $\delta^{15}N_{NO3}$ and $\delta^{18}O_{NO3}$,) will be used to reveal the potential biogeochemical processes related to the biogeochemical cycling of N, also, to provide useful information about the sources of NO_3^- as well as the impact of N cycling on As mobilization in groundwater systems.
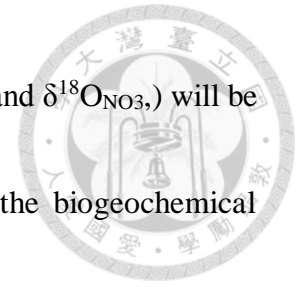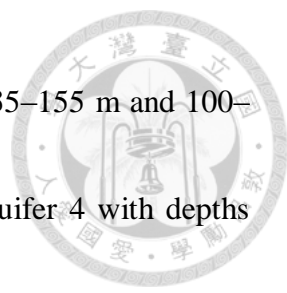
3. Study area

The Choushui River alluvial fan is located in southwestern Taiwan (Fig. 4a). The groundwater catchment of this region is surrounded by the Taiwan Strait (to the west) and the Central Mountain Range (to the east), and it is broadly partitioned into the proximal fan, mid-fan, and distal fan areas. Two major rivers flow through the alluvial fan: the Choushui River to the north and the Peikang River to the south.

On the basis of accelerator mass spectrometry ^{14}C (radiocarbon isotope) dating of mollusk shells in core samples of the Choushui River alluvial fan (Central Geological Survey, 1999), the geologic ages of core samples in the distal fan to the mid-fan could be grouped as follows: 2,931 to 5,364 yr, 7,090 to 9,230 yr, and older than 36,400 yr. Sedimentary formation was in the late Quaternary period and extended to a depth of approximately 300 m (Central Geological Survey, 1999). The shallow aquitard with depths of 0 to −55 m was deposited 3–9 ka ago during the Holocene transgression, the middle aquitard with depths of −100 to −155 m was deposited 35–50 ka ago, and the deep aquitard was deposited 80–120 ka ago. On the basis of subsurface hydrogeological analysis up to a depth of approximately 300 m, the hydrogeological environment is divided into four types of aquifers (Fig. 5): aquifer 1 with depths of 0–103 m, aquifer 2

15

with depths of 35–217 m (divided into 2-1 and 2-2 with depths of 35–155 m and 100–217 m, respectively), aquifer 3 with depths of 140–275 m, and aquifer 4 with depths exceeding 271 m (Central Geological Survey, available from http://hydro.moeacgs.gov.tw/). Fig. 5 shows that mud layer and gravel or sand bed cross from the top layer to the bottom layer; rock strata and mountain layer distribute from the inland area to the coastal area.

The watershed area of the Choushui River is 3,156.9 km^2 (Water Resources Agency, available from http://www.wra.gov.tw/). The annual average water quality of the Choushui River in 2015 is as follows: pH = 8.33, electrical conductivity (EC) = 506 μmho/cm, dissolved oxygen (DO) = 8.58 mg/L, NH_4^+ = 0.13 mg/L, total organic carbon (TOC) = 1.4 mg/L, NO_3^- = 3.89 mg/L, Mn = 0.482 mg/L, and As = 0.0031 mg/L (Environmental Protection Administration, available from http://www.epa.gov.tw/). The annual precipitation in the Choushui River alluvial fan is 1,972 mm in 2015, mostly concentrated in April to October (rainy season), and the historical yearly rainfall averages 2,366 mm (Water Resources Agency, available from http://gweb.wra.gov.tw/wrhygis/). The amount of irrigation area of the Choushui River alluvial fan is 47,680 ha, and the yearly irrigation water is 782.31 million ton (Water Resources Agency, available from
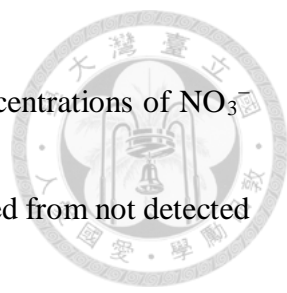
http://www.wracb.gov.tw/). The annual average temperature monitored by near climate

station is 24.3°C (Central Weather Bureau, Taiwan, available from

http://www.cwb.gov.tw/). The main land use of the Choushui River alluvial fan is for

agriculture, including rice cropping and upland farming, accounting for 60%, whereas the

main land use in the coastal area is for aquaculture (Fig. 6; Environmental Protection

Administration, 2014). The amount of fertilizer application in Taiwan is 347,039 ton,

including the N-containing fertilizers of 182,412 ton (Table 1; Council of Agriculture,

available from http://www.afa.gov.tw/). The average percentage of sewage permeating to

the Choushui River alluvial fan is 26.11% (Construction and Planning Agency, available

from http://www.cpami.gov.tw/). Hsu et. al (2013) reported that pumpage for non-

irrigation or irrigation purposes was regarded as known but illegal pumping was not

accounted for in the Choushui River alluvial fan. Recharge sources including rainfall,

rivers, boundary inflow, and groundwater irrigation have not been individually accounted

for in previous studies. However, Hsu et. al (2015) used groundwater storage hydrograph

and isotope analysis to estimate the pumpage and recharge of groundwater in the

Choushui River alluvial fan, and the result showed that the amount of yearly pumpage

for irrigation averaged 1.49 billion ton in 2012 to 2014, whereas that for non-irrigation

was 0.867 billion ton. The amounts of yearly average recharge from rainfall, rivers, boundary inflow, and groundwater irrigation were 0.796, 0.682, 0.879, and 0.377 billion ton, respectively. The yearly groundwater loss averaged 0.485 billion ton.
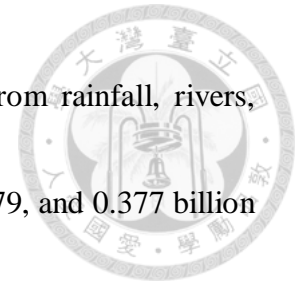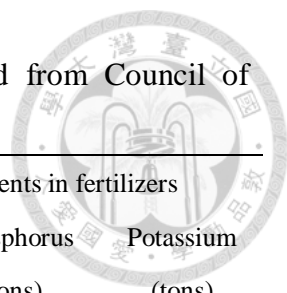
As, NO_3^-, and NH_4^+ are the target contaminants in the groundwater of the Choushui River alluvial fan. To frame a sound policy for remediation of groundwater contamination, it is crucial to determine the sources of contaminants and understand their biogeochemical cycling. The highest As concentration in sediments of the shallow aquifer of the Choushui River alluvial fan was found at a depth of approximately 50 m, where the deposits of the Holocene transgression are located (Liu et al., 2006). In 35% of the monitoring wells in the Choushui River alluvial fan, the As concentrations exceeded the World Health Organization guideline of 0.01 mg/L (Agricultural Engineering Research Center, 2012), with the highest As concentration being 0.96 mg/L (Agricultural Engineering Research Center, 2010). Lu et al. (2010) reported that the major As sinks and sources are As-bearing iron minerals and As-bearing sulfides, and authigenic framboidal pyrite commonly occurred in sediment of the Choushui River alluvial fan. Furthermore, in 76% of the monitoring wells, NH_4^+ concentrations exceeded the quality standard (0.1 mg/L) specified by the Taiwan Environmental Protection Administration for drinking water

18

sources (Agricultural Engineering Research Center, 2012). The concentrations of NO_3^- and NH_4^+ in the groundwater of the Choushui River alluvial fan ranged from not detected (ND) to 9.08 mg/L and from 0.02 to 15.6 mg/L, respectively (Kao et al., 2011). High concentrations of NO_3^- were found in the proximal fan, whereas high concentrations of NH_4^+ were mostly detected in the distal fan (Agricultural Engineering Research Center, 2012). Notably, NH_4^+ concentrations of shallow wells were greater than those of deep wells (Liu et al., 2003; Wang et al., 2007). The heterogeneous vertical distribution of NH_4^+ concentrations may be attributed to the frequent local agricultural use of N fertilizers or manure. Because groundwater pumping for crop irrigation is ubiquitous in the local region, overpumping of groundwater and anthropogenic activities have led to land subsidence and other adverse effects on the local environment.

The spatial distribution of NO_3^-, NH_4^+ contamination, and high As concentrations which occurred in the Choushui River alluvial fan may not be affected by a single process. They may be governed by multiple geochemical processes, including either the co-precipitation or the adsorption of the reduction products, or both, that control the mobilization of As into the reductive groundwater.

Table 1. Amount of fertilizer consumptions in Taiwan (modified from Council of Agriculture, available from http://www.afa.gov.tw/)

Fertilizer types	Consumption amount (tons)	Consumption rate of elements in fertilizers			
		Total (tons)	Nitrogen (tons)	Phosphorus (tons)	Potassium (tons)
Chemical fertilizers	1,010,722	347,039	182,412	65,039	99,588
ammonium sulfate	144,802	30,408	30,408	-	-
Diaminomethanal (Urea)	74,931	34,468	34,468	-	-
potassium chloride	27,565	16,539	-	-	16,539
calcium superphosphate	63,284	11,391	-	-	-
calcium ammonium nitrate	264	53	53	-	-
potassium	5,831	2,916	-	-	2,916
cyanide Calcium nitride	-	-	-	-	-
floats	115	-	-	-	-
compound fertilizer	679,091	251,264	117,483	53,648	80,133
others fertilizers	14,839	-	-	-	-
Organic fertilizers	100,401	-	-	-	-
animal and plant organic fertilizers	100,401	-	-	-	-
Total	1,111,123	347,039	182,412	65,039	99,588
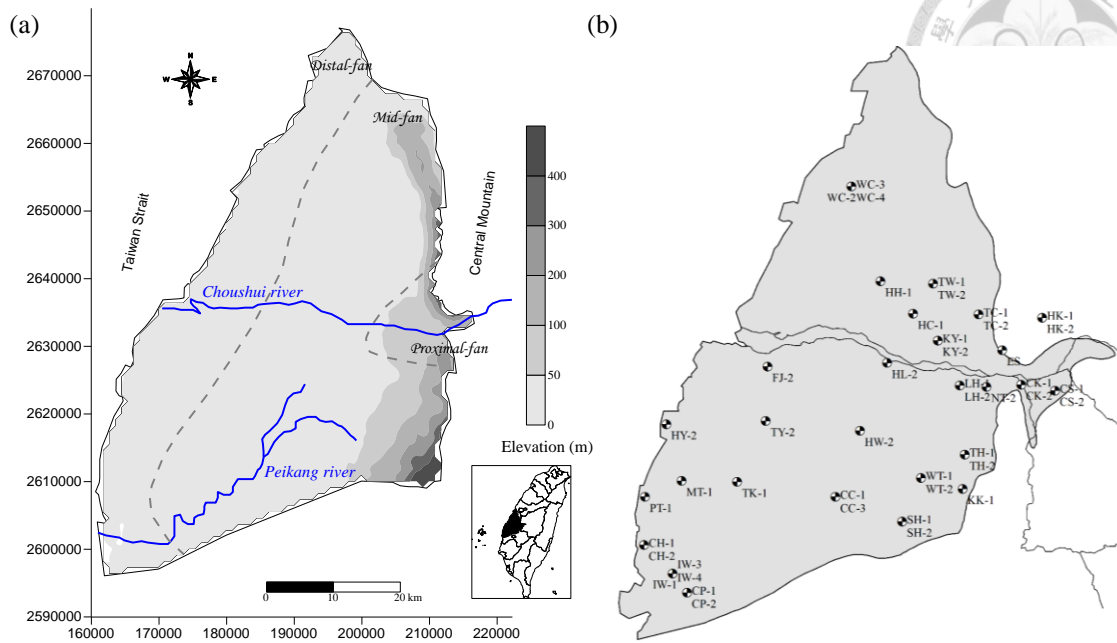
Fig. 4. (a) Study area and the division of the Choushui River alluvial fan into different fan regions. (b) Sampling locations of wells in the study area.
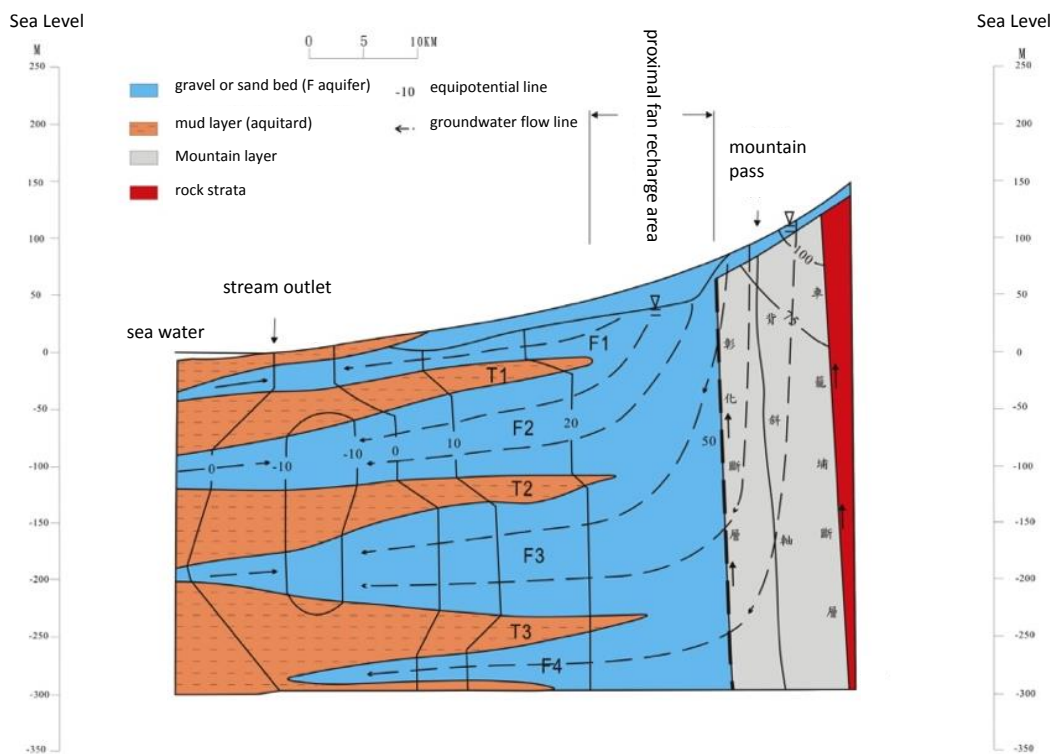
Fig. 5. Conceptual hydrogeological profile of the aquifer system in the Choushui River alluvial fan (modified from Central Geological Survey, 1986).

21
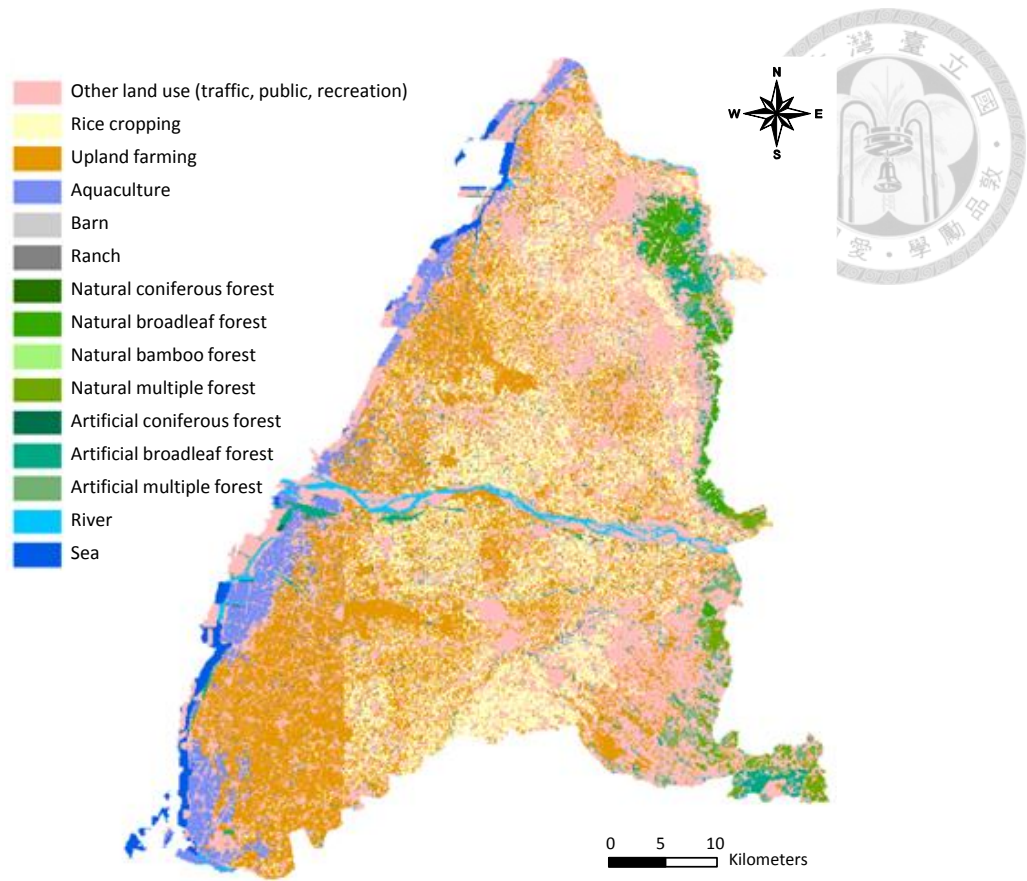
Fig. 6. Schematic for land use in the Choushui River alluvial fan (modified from Environmental Protection Administration, Taiwan, 2014).
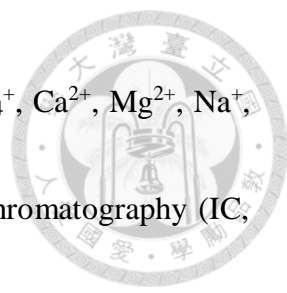
4. Materials and methods

In order to pursue the source of NO_3^- and NH_4^+ in groundwater of Choushui river alluvial fan, find the correlation between As and NH_4^+, identify the biogeochemical cycling of As, and elucidate the complex geochemical interaction between As and N, in this study, the mutltiple isotope analysis including δD and $\delta^{18}O_{H2O}$, $\delta^{15}N_{NO3}$ and $\delta^{18}O_{NO3}$ are applied. Therefore, the procedures of groundwater sampling, chemical analysis and multiple stable isotopes analysis indeed need to be well prepared.

4.1 Groundwater sampling and chemical analysis

46 groundwater samples were collected from 28 hydrological stations of Choushui river alluvial fan in September 2015 (Fig. 4b), including 21 shallow groundwater samples (depth ranges 0 to 100 m) and 25 deep groundwater samples (depth>100 m). All water samples were immediately filtered through 0.2 μm Mixed Cellulose Ester (MCE) membrane (ADVANTEC) after sampling, in order to analyze the hysical-chemical parameters (pH, temperature (T), dissolve oxygen (DO), oxidation-reduction potential (ORP, Eh), electrical conductivity (EC), total organic carbon (TOC), Cl^-, SO_4^{2-}, NO_3^-, NH_4^+, Ca^{2+}, Mg^{2+}, Na^+, K^+, Fe, Mn, and As), As species (As^{3+} and As^{5+}) and Fe species (Fe^{2+} and Fe^{3+}). All the physical-chemical analysis are execute in-situ or in the laboratory.

23
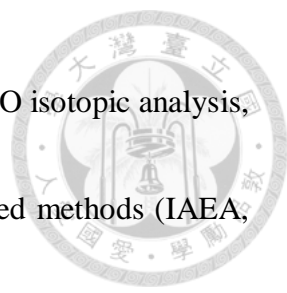
In all pretreated samples, dissolved Cl^-, SO_4^{2-}, NO_3^-, NO_2^-, NH_4^+, Ca^{2+}, Mg^{2+}, Na^+, and K^+ present in groundwater samples were determined by ion chromatography (IC, Dionex DX-120). Fe and Mn were determined by inductively coupled plasma optical emission spectrometry (ICP-OES, Varian VISTA-MPX). Concentrations of As were determined using an electro thermal atomic absorption spectrometer (AAS, Perkin-Elmer AA100) equipped with a hydride generation (HG, Perkin-Elmer FIAS100) system.

Concentrations of As species were analyzed by inductively coupled plasma mass spectrometer (ICP-MS, Agilent Technologies Agilent 7700x) equipped with high performance liquid chromatography (HPLC, Agilent 1260 Infinity Quaternary LC System). Ferrous concentration (Fe^{2+}) will be measured colorimetrically by spectrophotometer (Thermo GENESYS 20) using the FerroZine method.

The procedures of all chemical analysis followed the standard methods of USEPA or Environmental Analysis Laboratory of Taiwan EPA. The in-situ measurement and analytical results indeed provided geochemical conditions for designing laboratory experiments.

4.2 Multiple stable isotopes analysis

The groundwater samples were filtered through 0.2 µm MCE membrane, except

those for δD and $\delta^{18}O_{H2O}$ which were stored without filtering. For H_2O isotopic analysis,

the δD and $\delta^{18}O_{H2O}$ values were determined by using well-established methods (IAEA,

1983) on the high-precision isotopic water analyzer (PICARRO L2130-i) in the Institute

of Earth Sciences, Academia Sinica. The precision (1σ) is <25 per meg for $\delta^{18}O$ (<0.025

‰) and <100 per meg for δD (<0.1 ‰). Isotope data are reported as per mill (‰) relative

to the Vienna Standard Mean Ocean Water (V-SMOW) standard.

For nitrogen isotope analysis, filtered samples for $\delta^{15}N_{NO3}$ and $\delta^{18}O_{NO3}$ were frozen

immediately after sampling and stored in a -20℃ room in the laboratory until just before

analysis. The samples of $\delta^{15}N_{NO3}$ and $\delta^{18}O_{NO3}$ in NO_3^- were pre-treated according to the

bacterial denitrification method of Sigman et al. (2001). This method is to culture the

denitrifying bacteria (e.g., Pseudomonas chlororaphis and P. aureofaciens) that lack

nitrous oxide (N_2O) reductase, and thus N_2O from NO_3^- to nitrite (NO_2^-) and nitric oxide

(NO) will not free further to dinitrogen (N_2). The isotopes of N_2O are then analyzed. First,

we streaked with bacteria in prepared plates, followed by incubating the bacteria in

Tryptic Soy Broth (TSB). Within these steps, it was crucial to test the bacteria for

incomplete conversion of NO_3^-, in order to confirm the bacteria indeed convert NO_3^- to

N_2O, and stop by N_2O. After centrifugation to concentrate cell cultures, the bacteria were
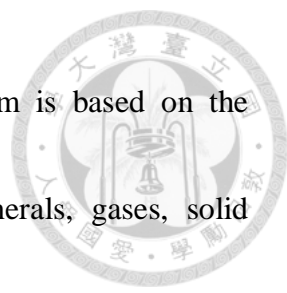
harvested. Sample vials added with concentrated cell cultures were injected with samples

of $\delta^{15}N_{NO3}$ and $\delta^{18}O_{NO3}$. The appropriate amount of samples is 1 to 10 mL. The $\delta^{15}N_{NO3}$

and $\delta^{18}O_{NO3}$ were analyzed on the continuous flow isotope ratio mass spectrometer (CF-

IRMS, Thermo Electron Delta V Advantage) in Graduate Institute of Hydrological and

Oceanic Sciences in National Central University and Research Center for Environmental

Changes in Academia Sinica. The precision (1σ) is <0.2 ‰.

The stable isotope analyses of $\delta^{15}N_{NO3}$ and $\delta^{18}O_{NO3}$ were helpful indicators in this

study of geochemical reactions and under varying redox conditions.

4.3 Nitrogen cycling process simulations

Major N cycling processes, including nitrification and denitrification, and the release

of As in the Choushui River alluvial fan were simulated in PHREEQC by using mainly

the physicochemical characteristics of groundwater, the concentrations of NO_3^-, NH_4^+,

As, and the values of $\delta^{15}N_{NO3}$.

PHREEQC, a public software developed by USGS and based on thermodynamic

databases, belongs to a sort of geochemical programs and is widely used to perform the

calculations and simulations of geochemical reactions and transport processes in natural

and polluted water, such as aqueous model, ion exchange, surface complexation, solid

26

solutions, transport modeling, and inverse modeling. The program is based on the

equilibrium chemistry of aqueous solutions interacting with minerals, gases, solid

solutions, exchangers, and sorption surfaces. The specific applications are mainly the

speciation calculations and reactive transport modeling to obtain SI for calcite in river

water and groundwater (Postma et al., 2007); the calculations of speciation, mineral

saturation indices (SI), and transfer coefficients for minerals selected in inverse

geochemical modeling (Sengupta et al., 2014); the speciation analysis of groundwater

samples (Hartland et al., 2015); the equilibration run for ionic concentrations (Mapoma

et al., 2016). PHREEQC can also model various 1-D transport processes including

diffusion, advection, and dispersion. These processes can be incorporated with

equilibrium and chemical kinetic reactions (Parkhurst and Appelo 1999).

In this study, PHREEQC Interactive 3.3.11, based on the thermodynamic databases

of imm.dat, phreeqc.dat, and iso.dat, was used to assess and simulate the speciation

concentrations of N compounds and the behavior of hydrogeochemical transport of N and

As in subsurface flow pathways in the Choushui River alluvial fan.
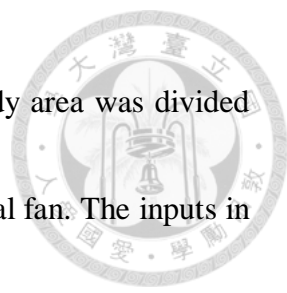
The concentrations of NO_3^- and NH_4^+ were collected to be the major inputs while

simulating N cycling processes, using default database of imm.dat for nitrification and
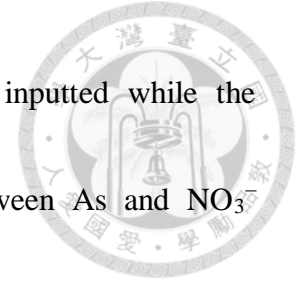
phreeqc.dat for denitrification. The concentrations of As were inputted while the simulations were evaluated toward deciphering the relation between As and NO_3^- denitrification.

While simulating the occurrence of nitrification, the data of pH, Temperature (°C), ORP (mV), and the concentrations of NO_3^- (mg/L), NH_4^+ (mg/L), DO (mg/L) were inputted, in order to provide the information for PHREEQC to determine the redox condition in groundwater environment. The built-in Amm.dat was selected as the database, and then Nitrification in Rates and Kinetics was set up as well.

By contrast, for denitrification simulations, the concentrations of CH_2O (mg/L), HCO_3^- (mg/L) needed to be inputted besides the aforesaid parameters. The built-in Phreeqc.dat was selected as the database. The concentrations of CH_2O calculated from TOC (mg/L) ×0.9 (Thurman, 1985) represented the carbon source for the usage of bacteria, and they were set up in codes of solution_master_species, solution_species, and reaction. The concentrations of HCO_3^- were assisted to calibrate the simulation result (chemical reaction equilibrium) referring to Eq. (3) of denitrification reaction equation. HCO_3^- is the final substance in NO_3^- denitrification reaction, obtaining from the analysis of physicochemical characteristics of groundwater in this study.

28
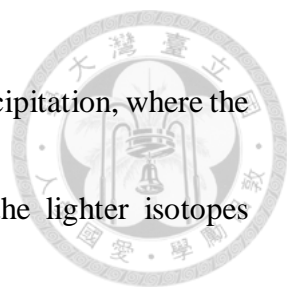
For 1-D transport of N compounds of NO_3^- and NH_4^+, the study area was divided

into three areas including the proximal fan, the mid-fan, and the distal fan. The inputs in

PHREEQC are pH, temperature, pe, DO (mg/L), Cl^- (mg/L), SO_4^{2-} (mg/L), NO_3^- (mg/L),

NH_4^+ (mg/L), S^{2-} (mg/L), HCO_3^- (mg/L), As (mg/L), and Fe (mg/L). The built-in

wateq4f.dat was selected as the database, and then Nitrification and denitrification in

Rates and Transport were both set up as well. The velocity of groundwater was set up as

0.01 m/day. The groundwater physicochemical characteristics of well NT-2, WT-1, and

HY-2 represent the areas of the proximal fan, the mid-fan, and the distal fan, respectively.

Moreover, the kinetic transport results of initial, one year, five years, ten years, and

twenty-five years were simulated simultaneously.

5. Results and discussion

5.1 Mixing of groundwater and extrinsic influences on groundwater
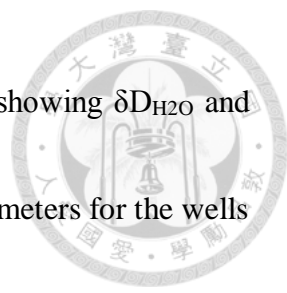
All the samples were classified into three categories on the basis of the location of their source wells: the proximal fan, mid-fan, and distal fan. The values of δD_{H2O} and $\delta^{18}O_{H2O}$ determined for the 46 groundwater samples are summarized in Table 2 and plotted in Fig. 7a. Fig. 7a shows the high δD_{H2O} and $\delta^{18}O_{H2O}$ values observed in the distal fan, the low δD_{H2O} and $\delta^{18}O_{H2O}$ values found in the proximal fan, and the average dispersion of the δD_{H2O} and $\delta^{18}O_{H2O}$ values in the mid-fan. The δD_{H2O} and $\delta^{18}O_{H2O}$ values in the groundwater range from $-72.92‰$ to $-21.93‰$ and from $-10.44‰$ to $-3.64‰$, respectively. The mean δD_{H2O} values in the groundwater in the proximal fan, mid-fan, and distal fan are $-8.27‰ \pm 0.83‰$ ($n = 23$), $-7.81‰ \pm 1.78‰$ ($n = 13$), and $-6.51‰ \pm 1.06‰$ ($n = 10$), respectively, and the mean $\delta^{18}O_{H2O}$ values in the groundwater in the proximal fan, mid-fan, and distal fan are $-56.53‰ \pm 6.91‰$ ($n = 23$), $-52.59‰ \pm 11.60‰$ ($n = 13$), and $-41.82‰ \pm 7.47‰$ ($n = 10$), respectively. The lowest hydrogen (H) and oxygen (O) isotope composition was observed at the sampling well KY-2 ($\delta D_{H2O} = -72.92‰$ and $\delta^{18}O_{H2O} = -10.44‰$), and the highest H and O isotope composition was found at the sampling well CH-1 ($\delta D_{H2O} = -21.93‰$ and $\delta^{18}O_{H2O} = -3.64‰$).

30

Ingraham (1998) explained the continental effect observed in precipitation, where the heavier isotopes of vapors precipitate near the coastal area and the lighter isotopes continue to fractionate and float toward the inland before they precipitate. Because groundwater is mostly accumulated through the infiltration of rainwater (meteoric water), it has isotopic signatures more or less the similar to those of local rainwater.

Fig. 7a shows the effect of mixing of upstream groundwater and downstream groundwater. The distributions of the δD_{H2O} and $\delta^{18}O_{H2O}$ values derived from the proximal fan, mid-fan, and distal fan are distinct and successive. The H and O isotope composition are lower in the groundwater samples of the proximal fan, and their value increases in the downstream direction, confirming the mixing of groundwater from the three fan regions.

The isotope analysis of δD_{H2O} and $\delta^{18}O_{H2O}$ showed that CH-1 had the highest δD_{H2O} and $\delta^{18}O_{H2O}$ values (−21.93‰ and −3.64‰, respectively). In Table 3, the EC is the highest in CH-1 among the 46 groundwater samples, reaching 21,750 μmho/cm; moreover, the Cl^- and SO_4^{2-} concentrations are also the highest in CH-1, reaching 7,470 mg/L and 1,150 mg/L, respectively. These observations indicate that CH-1 is influenced by seawater infiltration or intrusion resulting from aquaculture activity and overpumping

31
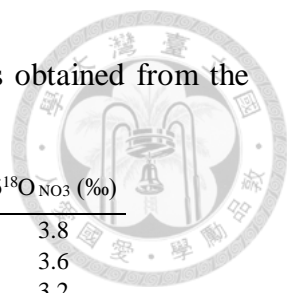
of groundwater. Kao et al. (2012) opined that the reason for KY-2 showing δD_{H2O} and

$\delta^{18}O_{H2O}$ values markedly lower than the average values of these parameters for the wells

in the proximal fan could be the lateral boundary influx from alluvial aquifers located

between the upstream region and the downstream region of the proximal fan. Furthermore,

Kao et al. (2011) suggested that the paleo-marine environment might be responsible for

the relatively higher δD_{H2O} and $\delta^{18}O_{H2O}$ values of CC-1; the high concentrations of EC,

Cl^-, and SO_4^{2-}, reaching 3,070 μmho/cm, 601 mg/L, and 344 mg/L, respectively, also

evidenced the existence of paleo-marine environment.

The meteoric water line of 46 groundwater samples can be formulated as $\delta D = 7.3$

$\delta^{18}O + 4.6$, and it is similar to the meteoric water line of the groundwater in the vicinity

of the Choushui Rive, which was reported as $\delta D = 8.1 \delta^{18}O + 13.8$ by Wang et al. (2000).

The slight offset between these two meteoric water lines can be explained by the effect

of a combination of various reactions related to evaporation, condensation, and

transportation in the local water (Sharp, 2007). Fig. 7b shows an inverse correlation of

EC versus depth (EC decreased with depth) in the aquifers of the proximal fan and the

mid-fan, suggesting the occurrence of evaporation or evapotranspiration, whereas there

is no obvious evaporation trend in the distal fan. The plot of EC versus SO_4^{2-} (Fig. 8h)

also shows significant evaporation or evapotranspiration in the mid-fan. CH-1 with the highest δD_{H2O} and $\delta^{18}O_{H2O}$ values and CC-1 with the second highest values attributed to seawater infiltration or intrusion and paleo-marine environment, respectively, were the main causes of offset between the two meteoric water lines. Kao et al. (2011) reported that $\delta^{18}O_{H2O}$ values of salinized groundwater were averagely greater than those of non-salinized groundwater, causing the meteoric water line to offset towards the right side against the original one.

33

Table 2. Results of isotope analysis of the 46 groundwater samples obtained from the Choushui River alluvial fan in 2015.

Region	Well name	δD$_{H2O}$ (‰)	δ^{18}O$_{H2O}$ (‰)	δ^{15}N$_{NO3}$ (‰)	δ^{18}O$_{NO3}$ (‰)
Proximal fan	TC-1	-62.21	-8.85	7.5	3.8
	TC-2	-59.36	-8.58	7.9	3.6
	ES	-56.57	-8.46	4.0	3.2
	TW-1	-58.48	-8.52	6.6	19.0
	TW-2	-61.52	-8.93	8.7	33.7
	KY-1	-64.09	-9.19	9.0	7.3
	KY-2	-72.92	-10.44	6.4	2.1
	CS-1	-56.71	-8.25	14.5	3.2
	CS-2	-49.11	-7.31	1.0	25.7
	CK-1	-47.39	-7.45	4.8	3.7
	CK-2	-47.03	-7.30	7.2	22.9
	WT-1	-50.56	-7.45	7.4	17.8
	WT-2	-49.72	-7.46	6.5	7.1
	TH-1	-55.60	-8.14	8.3	3.6
	TH-2	-53.55	-7.83	5.6	5.3
	LH-1	-66.03	-9.27	6.8	3.3
	LH-2	-64.48	-9.13	6.6	3.9
	NT-2	-65.16	-9.18	7.6	3.9
	SH-1	-53.08	-7.62	7.1	8.9
	SH-2	-51.00	-7.50	7.3	11.2
	KK-1	-51.05	-7.34	4.0	7.9
	HK-1	-51.81	-7.85	7.1	1.4
	HK-2	-52.81	-8.06	4.7	8.1
Mean	-	*-8.27*	*-56.53*	*6.80*	*9.16*
SD	-	*0.83*	*6.91*	*2.46*	*8.67*
Mid fan	WC-1	-41.36	-5.97	2.4	27.7
	WC-2	-62.68	-9.44	3.1	16.9
	WC-3	-63.56	-9.63	6.0	24.9
	WC-4	-63.99	-9.71	5.5	21.0
	HH-1	-38.26	-5.82	2.6	17.2
	HW-2	-55.10	-8.16	12.3	25.9
	HL-2	-57.63	-8.47	9.0	30.9
	CC-1	-27.21	-3.85	0.9	15.9
	CC-3	-49.43	-7.49	4.3	23.5
	FJ-2	-65.89	-9.60	10.2	34.1
	TY-2	-56.01	-8.41	5.7	10.3
	TK-1	-46.18	-6.88	13.4	30.5
	HC-1	-56.41	-8.06	3.3	20.3
Mean	-	*-7.81*	*-52.59*	*6.05*	*23.00*
SD	-	*1.78*	*11.60*	*3.98*	*6.88*
Distal fan	PT-1	-43.59	-6.80	9.7	30.2
	IW-1	-40.79	-6.30	6.6	9.3
	IW-3	-41.65	-6.63	10.9	27.0
	IW-4	-43.32	-6.95	9.8	28.7
	CH-1	-21.93	-3.64	15.3	18.7
	CH-2	-47.96	-7.35	12.9	32.0
	CP-1	-43.08	-6.45	13.5	19.5
	CP-2	-48.22	-7.29	9.6	19.4
	HY-2	-41.35	-6.70	9.4	25.5
	MT-1	-46.33	-6.97	11.1	25.3
Mean	-	*-6.51*	*-41.82*	*10.87*	*23.57*
SD	-	*1.06*	*7.47*	*2.47*	*6.85*

Table 3. Physical and chemical analysis results for the 46 groundwater samples collected from the Choushui River alluvial fan in September 2015.

Region	Well name	Well depth (m)	Water depth (m)	pH	Temp. (°C)	DO (mg/L)	ORP (mV)	EC (μmho/cm)	TOC (mg/L)	Cl^- (mg/L)	SO_4^{2-} (mg/L)	NO_3^- (mg/L)	NH_4^+ (mg/L)	Fe (mg/L)	Mn (mg/L)	As (mg/L)
Proximal fan	TC-1	140	13.56	7.09	24.4	3.81	95	770	0.4	9.6	109	22.98	0.05	0.018	ND<0.006	ND<0.0008
	TC-2	269	15.25	6.84	24.6	2.71	94	731	0.3	8.9	122	23.82	ND<0.01	0.023	ND<0.006	ND<0.0008
	ES	112.75	42.22	6.73	24.9	4.32	110	418	0.2	5.4	41.9	23.55	ND<0.01	0.015	ND<0.006	ND<0.0008
	TW-1	36	6.72	6.87	25.4	0.31	-120	1166	0.4	18.7	227	0.66	0.30	5.68	0.362	0.0068
	TW-2	244	18.7	7.54	24.8	0.01	-169	593	0.3	4.7	89.5	0.04	0.05	0.693	0.225	0.0027
	KY-1	38.7	11.14	6.85	24.8	0.05	-22	959	0.6	11.3	171	26.65	ND<0.01	0.033	0.081	ND<0.0008
	KY-2	97.55	11.39	7.22	24.9	2.12	20	759	0.4	4.7	174	10.23	ND<0.01	0.049	0.006	ND<0.0008
	CS-1	102.65	7.38	6.58	25.1	0.37	97	594	0.5	12.1	56.7	14.61	ND<0.01	0.029	0.145	ND<0.0008
	CS-2	199.3	6.92	7.43	25.1	0.01	29	372	0.4	0.65	3.6	0.04	0.18	0.084	0.19	0.0051
	CK-1	59	9.08	7.89	25.0	0.17	-71	417	0.4	3.4	26.6	0.04	0.05	0.103	0.055	ND<0.0008
	CK-2	150	5.08	8.03	25.4	0.03	-75	445	0.3	4.7	34.6	2.43	0.08	1	0.048	0.0008
	WT-1	35.67	5.82	6.85	24.2	0.13	-135	507	0.8	6.9	82.6	1.68	0.98	20.1	0.896	0.0168
	WT-2	101.25	4.43	6.34	24.9	0.92	12	407	0.2	9.6	71.3	24.61	0.01	0.025	ND<0.006	ND<0.0008
	TH-1	53.62	14.92	6.50	25.0	2.60	103	482	0.3	14.3	55.2	30.99	0.03	6.39	0.446	0.0017
	TH-2	120.6	15.28	6.47	25.0	2.20	110	407	0.2	9.6	26.2	25.68	0.10	0.064	ND<0.006	ND<0.0008
	LH-1	60.6	17.07	7.00	25.0	3.54	72	906	0.5	10.8	176	37.23	0.03	0.027	ND<0.006	ND<0.0008
	LH-2	114.1	17.24	7.21	24.7	3.60	83	754	0.3	8.4	142	22.67	ND<0.01	0.039	ND<0.006	ND<0.0008
	NT-2	96	31.98	7.06	25.1	4.69	80	840	0.5	8.9	159	27.80	0.12	0.034	ND<0.006	ND<0.0008
	SH-1	46.52	2.65	6.52	25.7	0.24	-112	620	0.6	24.4	68.8	28.95	0.49	6.5	0.45	0.0748
	SH-2	166.2	33.07	6.83	25.4	0.01	-144	232	0.3	5.4	16.6	0.49	ND<0.01	5.24	0.554	0.0024
	KK-1	109.8	39.56	6.21	24.5	6.52	123	410	0.3	11.3	59	60.65	0.03	0.053	ND<0.006	ND<0.0008
	HK-1	125.53	54.87	5.33	23.9	8.37	228	385	0.2	15	6.1	150.52	ND<0.01	0.04	ND<0.006	ND<0.0008
	HK-2	248.6	50	6.27	23.6	0.78	160	140	0.2	0.65	0.85	6.91	0.01	0.066	0.218	ND<0.0008
Mean	-	-	-	*6.85*	*24.84*	*2.07*	*25*	*579*	*0.37*	*9.10*	*83.5*	*23.62*	*0.17*	*2.01*	*0.28*	*0.01*
SD	-	-	-	*0.58*	*0.49*	*2.34*	*110*	*248*	*0.15*	*5.55*	*65.1*	*31.60*	*0.26*	*4.55*	*0.25*	*0.03*
Mid fan	WC-1	25	2.25	6.93	24.9	0.03	-128	1650	1.3	63.8	491	0.58	1.26	8.05	0.569	0.0467
	WC-2	68	6.59	7.38	25.2	0.02	-185	717	0.6	2.2	108	0.22	1.52	1.67	0.157	0.0036
	WC-3	128	8	7.53	25.7	0.16	-170	666	0.4	2.2	103	0.04	0.23	0.728	0.307	0.0043
	WC-4	212	8.96	7.61	27.3	0.09	-161	635	0.3	0.65	118	0.04	0.13	0.413	0.251	0.0046
	HH-1	23	5.12	6.75	25.7	0.01	-127	2049	0.6	46.6	765	1.15	0.28	13.9	0.385	0.0133
	HW-2	120.15	12.72	7.54	25.3	0.01	-169	593	0.2	17	256	0.44	0.12	4.2	0.257	0.0044
	HL-2	102	8.67	7.55	25.0	0.01	-313	640	0.2	5.5	111	0.09	0.05	1.35	0.214	0.0027
	CC-1	36.05	3.28	6.88	25.5	0.03	-168	3070	1.9	601	344	1.51	3.12	12.3	0.384	0.284
	CC-3	111.5	18.7	6.94	25.5	0.01	-179	439	2	4.2	5.2	0.62	2.94	6.1	0.226	0.146
	FJ-2	101	8.5	7.51	25.7	0.01	-165	591	0.4	4.7	102	0.09	0.46	0.92	0.16	0.0014
	TY-2	75.08	9.55	-	-	-	-	-	1.8	8.4	2	0.89	7.08	0.512	0.129	ND<0.0008
	TK-1	33	4.95	6.91	26.1	0.02	-118	1595	0.9	33	15.8	0.53	3.49	8.23	0.313	0.0702
	HC-1	32	7	6.91	25.3	0.03	-156	1485	0.4	22.7	423	0.66	0.21	7.46	0.516	0.0078
Mean	-	-	-	*7.20*	*25.60*	*0.04*	*-170*	*1178*	*0.85*	*62.46*	*218.8*	*0.53*	*1.61*	*5.06*	*0.30*	*0.05*
SD	-	-	-	*0.34*	*0.63*	*0.05*	*50*	*805*	*0.67*	*162.99*	*228.4*	*0.45*	*2.07*	*4.66*	*0.14*	*0.09*
Distal fan	PT-1	66.38	5.58	7.58	26.2	0.01	-236	4090	1.2	1210	124	0.49	10.11	6.27	0.765	0.317
	IW-1	96	19.92	7.44	26.7	0.09	-194	9380	1.5	2880	220	0.31	10.21	1.94	0.11	0.0387
	IW-3	219	23.53	7.91	29.7	0.15	-206	5670	1.1	1700	133	0.13	4.60	0.682	0.076	0.0194
	IW-4	261	20.22	8.24	31.1	0.01	-214	493	1.3	3	2.6	0.04	0.79	0.17	0.038	0.0089
	CH-1	56.37	4.33	7.52	26.5	0.02	-216	21750	0.5	7470	1150	0.44	10.03	3.13	0.065	0.0606
	CH-2	147.42	19.47	7.90	28.6	0.03	-262	1196	0.6	230	23	0.04	1.07	1.41	0.095	0.17
	CP-1	79.8	22.81	7.54	26.6	0.01	-215	10750	1.5	3800	202	0.18	18.29	1.21	0.292	0.25
	CP-2	173.8	24.81	7.77	29.0	0.01	-242	1100	0.9	215	19.7	0.18	1.70	1.08	0.16	0.0942
	HY-2	104.9	11.65	7.54	26.5	0.02	-223	1570	1.8	321	26.5	0.44	4.62	0.963	0.117	0.0191
	MT-1	56	10.68	7.73	25.9	0.01	-229	1172	1.9	79.6	21.3	0.22	5.44	2.06	0.269	0.503
Mean	-	-	-	*7.72*	*27.68*	*0.04*	*-224*	*5717*	*1.23*	*1790.86*	*192.2*	*0.25*	*6.69*	*1.89*	*0.20*	*0.15*
SD	-	-	-	*0.25*	*1.78*	*0.05*	*19*	*6711*	*0.47*	*2381.09*	*346*	*0.16*	*5.49*	*1.74*	*0.22*	*0.16*
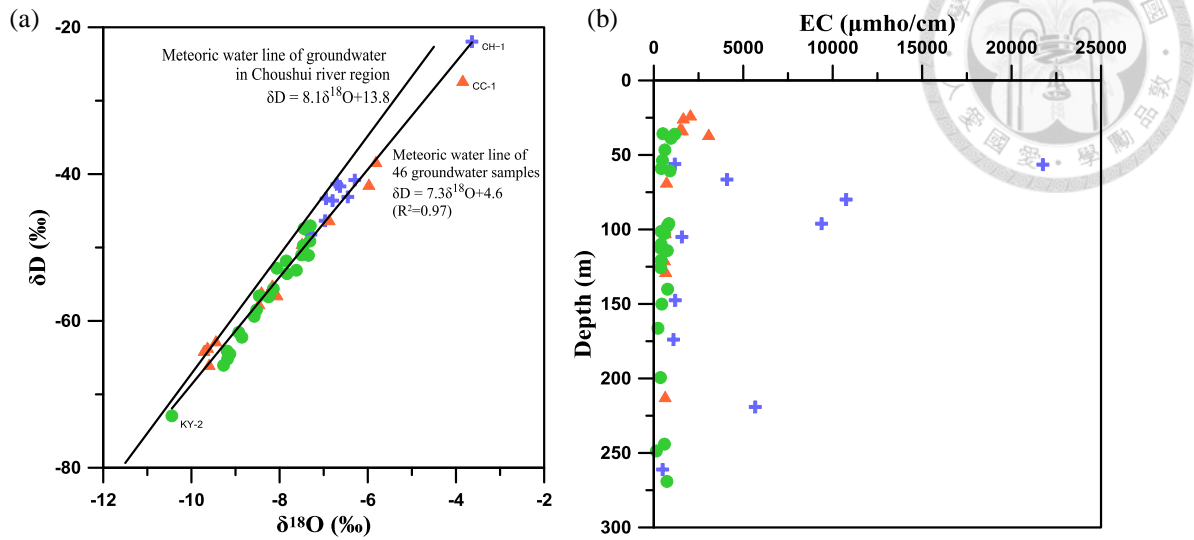
Fig. 7. (a) Plot of δD_{H2O} versus $\delta^{18}O_{H2O}$ for the 46 groundwater samples. (b) Plot of EC versus depth for the 46 groundwater samples. ●: proximal fan; ▲: mid fan; ✚: distal fan.
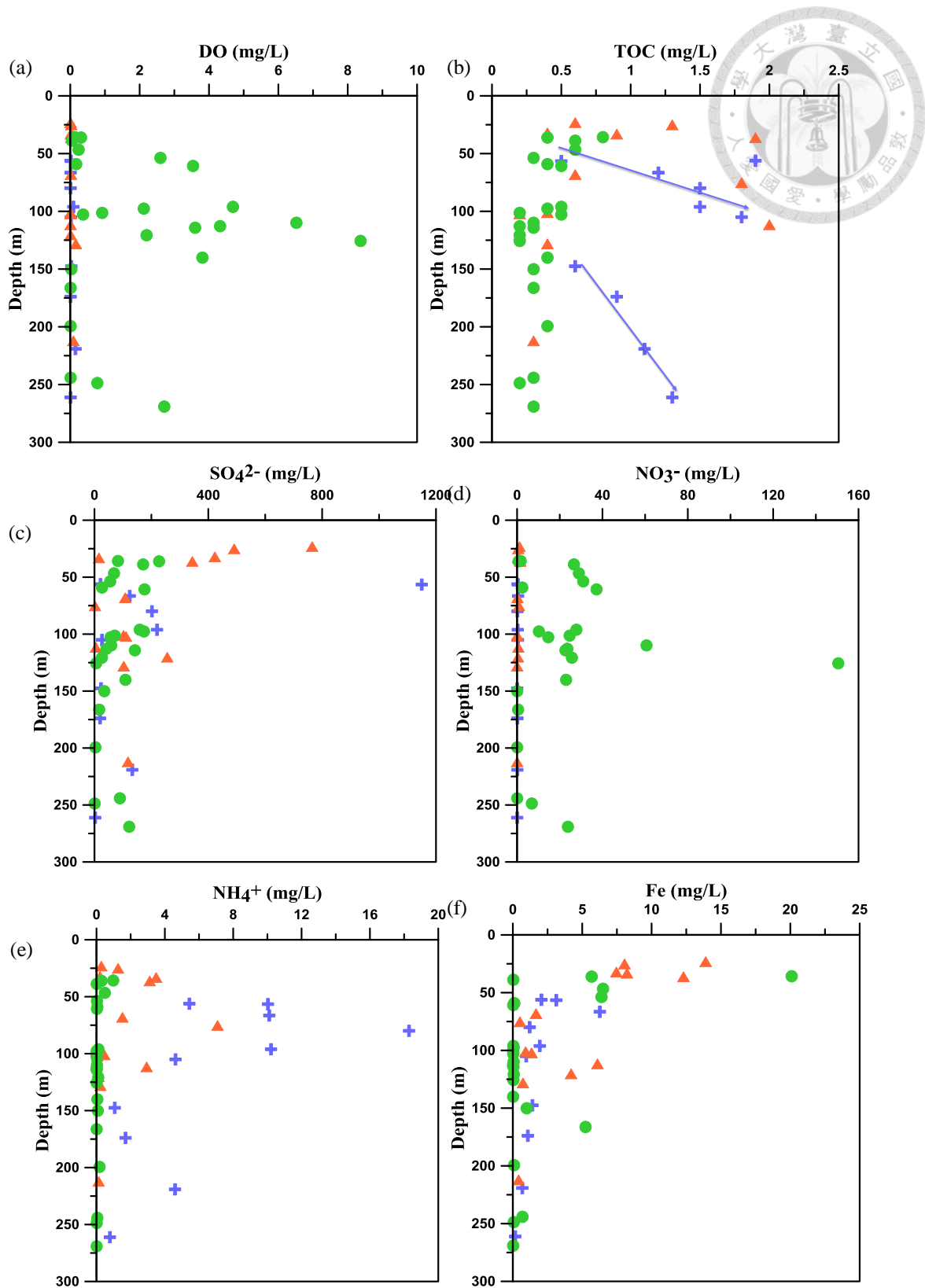
Fig. 8. Plots of depth versus water quality parameters and the relations between parameters for the 46 groundwater samples. ●: proximal fan; ▲: mid fan; +: distal fan.
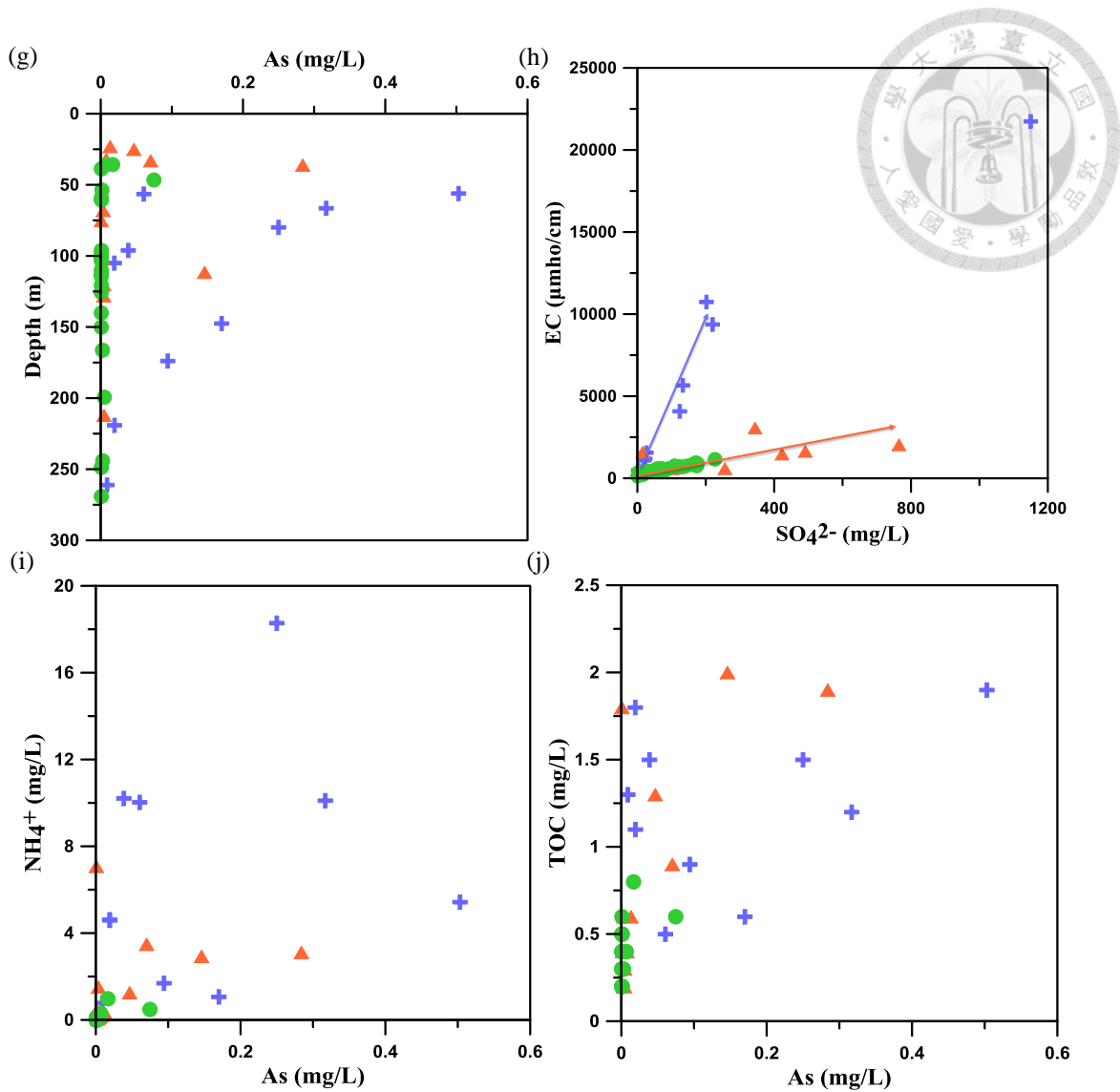
Fig. 8. (*Cont'd*)

5.2 Physicochemical characteristics of groundwater
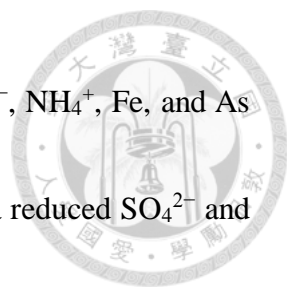
The results of the physical and chemical analyses are summarized in Table 3. Fig. 8

plots groundwater depth versus target water quality parameters and the relations between

parameters. Fig. 8a and the ORP value in Table 3 indicate that the groundwater in the

proximal fan tended to be highly oxidative, whereas the mid-fan and the distal fan were

under reductive state. Low ORP and low DO in the distal fan indicate that the groundwater

was anaerobic or under comparatively reduced conditions (Kao et al., 2011; Kurosawa et al., 2008).

Fig. 8a, 8b, 8c, 8d, and 8f show that the concentrations of DO, TOC, NO_3^-, SO_4^{2-}, and Fe decreased with depth in the proximal fan, whereas DO, NO_3^-, and SO_4^{2-} elevated in the depth of from 25 to 150 m and from 250 to 275 m. Kao et al. (2011) suggested that the recharge of meteoric water and extensive pumping of groundwater for agricultural requirement led to the entry of atmospheric O_2 into unconfined granular aquifers of the proximal fan, changing the reductive groundwater to be oxidizing state, or even complex redox condition. Fe and As concentrations remained low in aforementioned depth, which may be attributed to the co-precipitation or adsorption of As on Fe oxyhydroxides (Pierce and Moore, 1982; Peterson and Carpenter, 1983).
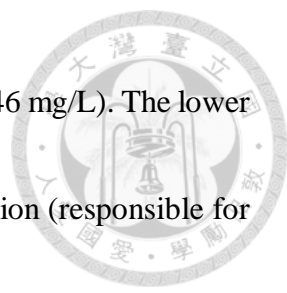
In the mid-fan, Fe, As, and SO_4^{2-} increased near surface of upper 50 m (Fig. 8c, 8f, and 8g), implying that the reductive dissolution of As-containing Fe oxyhydroxides resulted in the release of As into the groundwater, and meanwhile the oxidation of pyrite might also cause the As release in the complex redox environment. High concentrations of NH_4^+ in the upper 50 m (Fig. 8e) suggest that the N sources may be NH_4^+ fertilizers, manure, sewage water, or other transformation products (e.g., DNRA from NO_3^- sources),

39

which were evidenced by N and O isotope composition. TOC, SO_4^{2-}, NH_4^+, Fe, and As

decreased with depth, suggesting that when sulfate-reducing bacteria reduced SO_4^{2-} and

the oxidation of iron occurred, the production of sulfide minerals (e.g., FeS) and ferric

oxides subsequently precipitated As, adsorbed or co-precipitated aqueous As, lowering

As concentration in groundwater (Akai et al., 2004; Kirk et al., 2004; Swartz et al., 2004).

Similar situation occurred in the distal fan; however, TOC concentrations increased

with depth, forming two separate trends (Fig. 8b). High TOC in the upper zone of the

aquifer may be the result of the application of manure or the presence of septic waste and

livestock, and the deeper zone may be attributed to local geologic sediments.

Fig. 8h indicates that there are two distinct trends of EC versus the concentrations of

SO_4^{2-} in the mid-fan and the distal fan. The upper trend in the distal fan may be related

to seawater infiltration or intrusion. Wang et al. (2007) and Kao et al. (2011) reported the

occurrence of salinization in the southwestern coastal area of Taiwan and the average EC

value of salinized groundwater was greater than that of non-salinized groundwater.

Seawater infiltration and intrusion into the coastal area of the Choushui River alluvial fan

was verified by ^{18}O mass balance calculation, resulting in elevation of EC and SO_4^{2-} in

the distal fan. Also, the average concentration of Cl^- in the distal fan (1790.86 mg/L) was
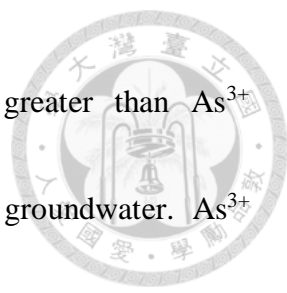
greater than that in the proximal fan (9.10 mg/L) and the mid-fan (62.46 mg/L). The lower

trend in the mid-fan may be related to evaporation or evapotranspiration (responsible for

elevation of EC) and pyrite oxidation (responsible for elevation of SO_4^{2-}), or paleo-

marine environment (responsible for elevation of both). Kao et al. (2011) suggested that

the mid-fan of the Choushui River alluvial fan was under the paleo-marine environment,

and this may contribute to the elevation of EC and SO_4^{2-}.

Moreover, Fig. 8d clearly shows that high NO_3^- concentrations were found in the

oxidative proximal fan, whereas low NO_3^- concentrations were observed in the reductive

distal fan. On the contrary, the As concentrations increased from the proximal to the distal

fan (Fig. 8g). Fig. 8i shows the plot of As versus NH_4^+ concentrations. The relationship

between As and NH_4^+ is not clear. Due to a sequence of complex redox processes, the

concentration correlation between As and NH_4^+ may not be confirmed without any further

evidence. Fig. 8j indicates a positive correlative relationship between As concentrations

and TOC, and as TOC increases, As increases. Redox conditions are controlling As

solubility. Because both nitrate and ferric iron are electron acceptors, the bacteria utilizing

them are essentially competing against one another. Denitrification is more

thermodynamically favored and thus its occurrence may actually be consuming electron

41

donors (i.e., organic matter) more rapidly and making them less available for iron reducing bacteria. The organic matter may be a more important control on redox conditions and thus As concentrations, as other studies have shown (Liu et al., 2003; Anawar et al., 2013). Many studies have reported the positive correlation between As and TOC because TOC implies the organic substrates for the requirement of reaction of As release from Fe oxyhydroxides into groundwater (Farooq et al., 2010; Hsu et al., 2010; Anawar et al., 2013; Pi et al., 2015; Lu et al., 2016). Notably, a spatial positive correlation is evident by As, NH_4^+, and TOC in Fig. 9. Elevated concentrations of As, NH_4^+, and TOC were mostly observed in the mid to distal fan of the Choushui River alluvial fan, which was opposite to the trend in NO_3^- concentrations. The samples of MT-1, PT-1, and CP-1 contained relatively high TOC and NH_4^+ concentrations as well as high As concentrations (Table 3). These sampling wells are located in the distal fan (Fig. 4b), where the groundwater is in a reductive state. CH-1 and IW-1 contained high NH_4^+ concentrations and relatively low As concentrations, which may be explained by the intrusion of manure, septic waste, or organic waste, and subsequent mineralization without triggering the release of As (Kurosawa et al., 2008).

Table 4 shows the As species analysis results. As^{5+} concentrations in four sampling

wells (KY-1, CS-2, CK-1, SH-1) of the proximal fan were greater than As^{3+}

concentrations, caused by the relatively oxidizing condition of groundwater. As^{3+}

concentrations in all wells of the mid-fan and the distal fan were distinctly greater than

As^{5+} concentrations because the groundwater was in reducing state. The concentrations

of Fe^{2+} (observed more in the reductive groundwater) and Fe^{3+} (observed more in the

oxidative groundwater) show similar behavior.

Table 5 presents a correlation analysis between the physical and chemical parameters.

The correlation of the NH_4^+ concentration with NO_3^-, ORP, and DO was statistically

significant. Specifically, NH_4^+ concentrations showed significant moderate-to-high

negative correlations with NO_3^-, ORP, and DO, with the correlation coefficients being

-0.511, -0.752, and -0.568, respectively. This suggests that the NH_4^+ concentration

increased in reductive conditions, thereby causing the NO_3^- concentration to decrease

through denitrification or dissimilatory NO_3^- reduction to NH_4^+ (DNRA).

As concentrations showed significant moderate-to-high negative correlations with

NO_3^-, the ORP, and DO, with correlation coefficients of -0.514, -0.777, and -0.658,

respectively. This suggests that the release of As from sediments may increase when the

groundwater becomes more reductive, and denitrification or DNRA may occur

43
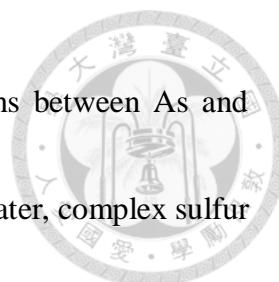
simultaneously with As release. The lack of significant correlations between As and

SO_4^{2-} also suggests that in the reductive environment of the groundwater, complex sulfur

disproportionation geochemical processes control the As concentration in the

groundwater (Kao et al., 2011). Kirk et al. (2004) show that sulfate reduction can be an

important limit on As in solution; i.e., the production of sulfide removes As from solution.

Sulfate and As thus tend to have a "mutually exclusive" relationship, and our data in this
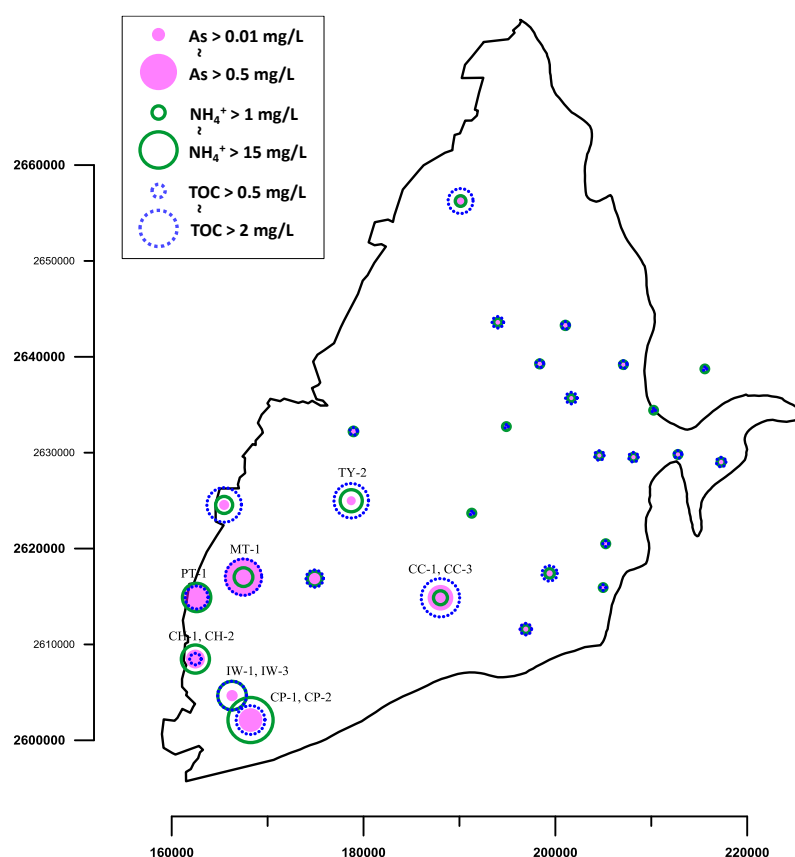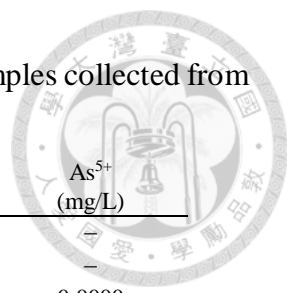
study generally show this relationship.

Fig. 9. Plots of spatial distribution of As, NH_4^+, and TOC for the 46 groundwater samples.

44

Table 4. Fe and As species analysis results for the 46 groundwater samples collected from the Choushui River alluvial fan in September 2015.

| Region	Well name	Fe^{2+} (mg/L)	Fe^{3+} (mg/L)	As^{3+} (mg/L)	As^{5+} (mg/L)
Proximal fan	TC-1	0.301	0.206	−	−
	TC-2	0.352	0.258	−	−
	ES	0.301	0.361	0.0000	0.0000
	TW-1	17.7	0.000	0.0072	0.0006
	TW-2	2.00	0.619	0.0031	0.0000
	KY-1	0.301	0.206	0.0003	0.0006
	KY-2	0.352	0.516	−	−
	CS-1	0.352	0.361	−	−
	CS-2	0.301	0.309	0.0020	0.0045
	CK-1	0.765	0.516	0.0004	0.0006
	CK-2	0.765	0.206	0.0006	0.0003
	WT-1	64.1	0.773	0.0241	0.0033
	WT-2	0.507	0.052	−	−
	TH-1	0.455	0.103	0.0000	0.0000
	TH-2	0.558	0.000	−	−
	LH-1	0.404	0.103	−	−
	LH-2	0.713	0.103	−	−
	NT-2	0.455	0.412	−	−
	SH-1	8.24	1.34	0.0091	0.0329
	SH-2	13.6	3.35	0.0018	0.0008
	KK-1	0.713	0.000	−	−
	HK-1	0.558	0.000	−	−
	HK-2	0.610	0.206	−	−
Mid fan	WC-1	12.8	1.13	0.0310	0.0023
	WC-2	0.765	0.619	0.0031	0.0002
	WC-3	0.404	0.000	0.0043	0.0001
	WC-4	0.558	0.103	0.0047	0.0000
	HH-1	46.9	0.000	0.0151	0.0015
	HW-2	13.9	0.000	0.0041	0.0002
	HL-2	3.39	0.825	0.0027	0.0000
	CC-1	38.8	2.89	0.0181	0.0029
	CC-3	19.1	2.06	0.1736	0.0147
	FJ-2	0.765	0.773	0.0016	0.0003
	TY-2	0.661	0.619	−	−
	TK-1	26.5	0.000	0.0985	0.0115
	HC-1	23.8	0.000	0.0090	0.0003
Distal fan	PT-1	12.3	5.36	0.0162	0.0028
	IW-1	4.79	1.34	0.0485	0.0071
	IW-3	0.816	0.000	0.0274	0.0022
	IW-4	0.971	0.155	0.0115	0.0008
	CH-1	6.80	2.84	0.0602	0.0128
	CH-2	1.07	0.309	0.1687	0.0123
	CP-1	2.11	1.13	0.0157	0.0033
	CP-2	1.33	0.412	0.1368	0.0075
	HY-2	1.02	0.928	0.0261	0.0052
	MT-1	0.765	0.412	0.0312	0.0042
	TK-1	26.5	0.000	0.0985	0.0115
	HC-1	23.8	0.000	0.0090	0.0003
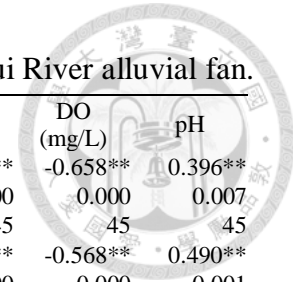
Table 5. Correlations between the physical and chemical analysis results for the 46 groundwater samples of the Choushui River alluvial fan.

Spearman's rho coefficient		As (mg/L)	NH$_4^+$ (mg/L)	NO$_3^-$ (mg/L)	SO$_4^{2-}$ (mg/L)	Fe (mg/L)	Mn (mg/L)	TOC (mg/L)	EC (μmho/cm)	ORP (mV)	DO (mg/L)	pH
As (mg/L)	Correlation coefficient	1.000	0.817**	-0.514**	0.130	0.765**	0.356*	0.679**	0.590**	-0.777**	-0.658**	0.396**
	Significance	.	0.000	0.000	0.387	0.000	0.033	0.000	0.000	0.000	0.000	0.007
	Sample number	46	46	46	46	46	36	46	45	45	45	45
NH$_4^+$ (mg/L)	Correlation coefficient		1.000	-0.511**	0.091	0.616**	0.061	0.782**	0.631**	-0.752**	-0.568**	0.490**
	Significance		.	0.000	0.549	0.000	0.726	0.000	0.000	0.000	0.000	0.001
	Sample number		46	46	46	46	36	46	45	45	45	45
NO$_3^-$ (mg/L)	Correlation coefficient			1.000	0.069	-0.325*	0.260	-0.246	-0.209	0.754**	0.745**	-0.791**
	Significance			.	0.651	0.028	0.125	0.099	0.168	0.000	0.000	0.000
	Sample number			46	46	46	36	46	45	45	45	45
SO$_4^{2-}$ (mg/L)	Correlation coefficient				1.000	0.189	0.195	0.061	0.647**	-0.140	0.047	0.035
	Significance				.	0.207	0.254	0.688	0.000	0.358	0.761	0.819
	Sample number				46	46	36	46	45	45	45	45
Fe (mg/L)	Correlation coefficient					1.000	0.734**	0.438**	0.365*	-0.525**	-0.57**	0.105
	Significance					.	0.000	0.002	0.014	0.000	0.000	0.493
	Sample number					46	36	46	45	45	45	45
Mn (mg/L)	Correlation coefficient						1.000	0.005	0.068	0.089	-0.085	-0.498**
	Significance						.	0.977	0.696	0.613	0.627	0.002
	Sample number						36	36	35	35	35	35
TOC (mg/L)	Correlation coefficient							1.000	0.657**	-0.569**	-0.423**	0.347*
	Significance							.	0.000	0.000	0.004	0.020
	Sample number							46	45	45	45	45
EC (μmho/cm)	Correlation coefficient								1.000	-0.538**	-0.234	0.358*
	Significance								.	0.000	0.121	0.016
	Sample number								45	45	45	45
ORP (mV)	Correlation coefficient									1.000	0.775**	-0.733**
	Significance									.	0.000	0.000
	Sample number									45	45	45
DO (mg/L)	Correlation coefficient										1.000	-0.540**
	Significance										.	0.000
	Sample number										45	45
pH	Correlation coefficient											1.000
	Significance											.
	Sample number											45

Spearman's rank correlation is used to calculate the correlation coefficient; **: *p* value < 0.01; *: *p* value < 0.05

46

5.3 Sources and transformation of nitrogen in groundwater
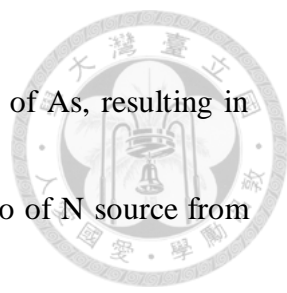
5.3.1 Probable sources of NO_3^-

The $\delta^{15}N_{NO3}$ and $\delta^{18}O_{NO3}$ values obtained from the 46 groundwater samples are presented in Table 2. All the analyzed water samples showed a compositional range between +0.9‰ and +15.3‰ for $\delta^{15}N_{NO3}$ and between +1.4‰ and +34.1‰ for $\delta^{18}O_{NO3}$. The $\delta^{15}N_{NO3}$ value ranges from +1.0‰ to +14.5‰, with a mean of 6.80‰ ± 2.46‰, in the proximal fan; from +0.9‰ to +13.4‰, with a mean of 6.05‰ ± 3.98‰, in the mid-fan; and from +6.6‰ to +15.3‰, with a mean of 10.87‰ ± 2.47‰, in the distal fan. Furthermore, the $\delta^{18}O_{NO3}$ value falls in the range of +1.4‰ to +33.7‰, with a mean of 9.16‰ ± 8.67‰, in the proximal fan; +10.3‰ to +34.1‰, with a mean of 23‰ ± 6.88‰, in the mid-fan; and +9.3‰ to +32.0‰, with a mean of 23.57‰ ± 6.85‰, in the distal fan.

Fig. 10 shows a plot of $\delta^{15}N_{NO3}$ versus $\delta^{18}O_{NO3}$. In particular, the $\delta^{18}O_{NO3}$ value is low in most groundwater samples of the proximal fan. This observation can be interpreted as reflecting the existence of oxygen sources other than NO_3^- in the groundwater (e.g., atmospheric O_2), resulting in microbes preferably using the other oxygen sources for biological reactions. High DO concentrations in the deeper aquifer were found in the proximal fan (Fig. 8a). Kao et al. (2011) suggested that the recharge of meteoric water

47

and anthropogenic activity of extensive pumping of groundwater for agricultural purposes led to the entry of atmospheric O_2 into unconfined granular aquifers, altering the redox conditions in the Choushui River alluvial fan.

NO_3^- in groundwater generally originates from various sources, including contaminated precipitation, nitrous fertilizers, and oxidation of dissolved NH_4^+. NO_3^- isotope ratios ($\delta^{15}N_{NO3}$ and $\delta^{18}O_{NO3}$) have recently been used to identify sources of NO_3^- and assess the occurrence of denitrification (Deutsch et al., 2006; Hosono et al., 2011; Umezawa et al., 2009). Fig. 11 shows the ranges of NO_3^- isotope ratios for possible source materials; the ranges of some sources overlap. The $\delta^{15}N_{NO3}$ and $\delta^{18}O_{NO3}$ values in groundwater samples of the distal fan and the mid-fan of the Choushui River alluvial fan mostly fall between the ranges for atmospheric deposits (NO_3^-), nitrate fertilizers, and marine nitrate, indicating that the N and O isotope composition might originate from a combination of these sources; a few values of the isotope ratios directly fall in the range of nitrate fertilizers, revealing that the main constituent of fertilizers used in the distal fan and the mid-fan is NO_3^-. Fig. 11 also suggests that the NO_3^- sources of IW-1 may be the transformation of manure or septic waste, indicating that the original source is organic waste and NH_4^+, which is present in high concentration. Kurosawa et al. (2008) observed

48

that the mineralization of organic waste may not trigger the release of As, resulting in relatively low As concentration being maintained. However, the ratio of N source from atmosphere may be too low to affect N to the system, whereas the N source of marine nitrate seems to have some contribution as a consequence of the paleo-marine environment and seawater infiltration or intrusion caused by aquaculture activity and groundwater overpumping (evidenced by the concentrations of EC, Cl^-, and SO_4^{2-} of the wells of CC-1 and CH-1). The mixing ratio yet requires further investigation due to the lack of $\delta^{15}N$ values of end sources (Caldwell, 1998; Mariotti et al., 1988; Pauwels et al., 2000; Seiler, 2005). The NO_3^- isotope ratios in the proximal fan fall in the compositional fields of ammonium fertilizers, soil ammonium, marine nitrate, and manure and septic waste, indicating that either agricultural activities in the proximal fan mainly involved NH_4^+ fertilizers and manure or the groundwater is contaminated by septic waste. In the groundwater in the proximal fan, NH_4^+ is oxidized to NO_3^- (nitrification) in the oxidative environment, resulting in NO_3^--enriched groundwater. By contrast, agricultural activities in the mid-fan and the distal fan mainly involve the use of NO_3^- fertilizers, and the NO_3^- is reduced to either other phases of NO_2^-, NO, N_2O, and N_2 (denitrification) or to NH_4^+ through DNRA in the reductive environment.
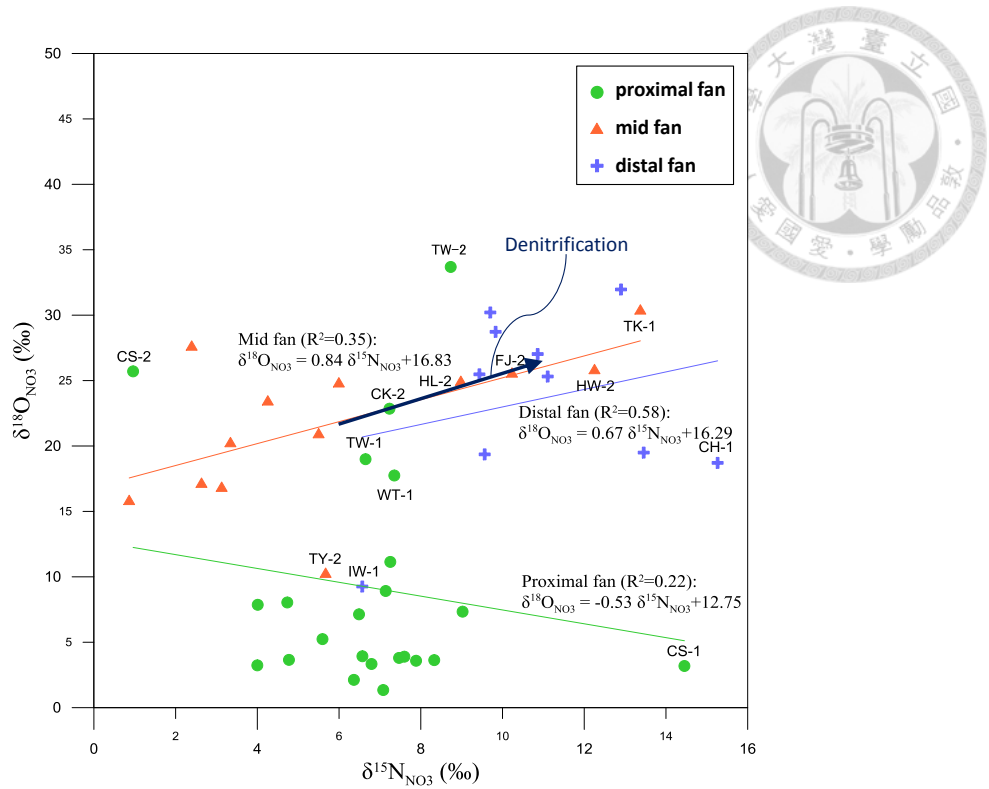
Fig. 10. Plot of $\delta^{15}N_{NO3}$ versus $\delta^{18}O_{NO3}$ showing the denitrification trend and formulated relationship for the 46 groundwater samples.
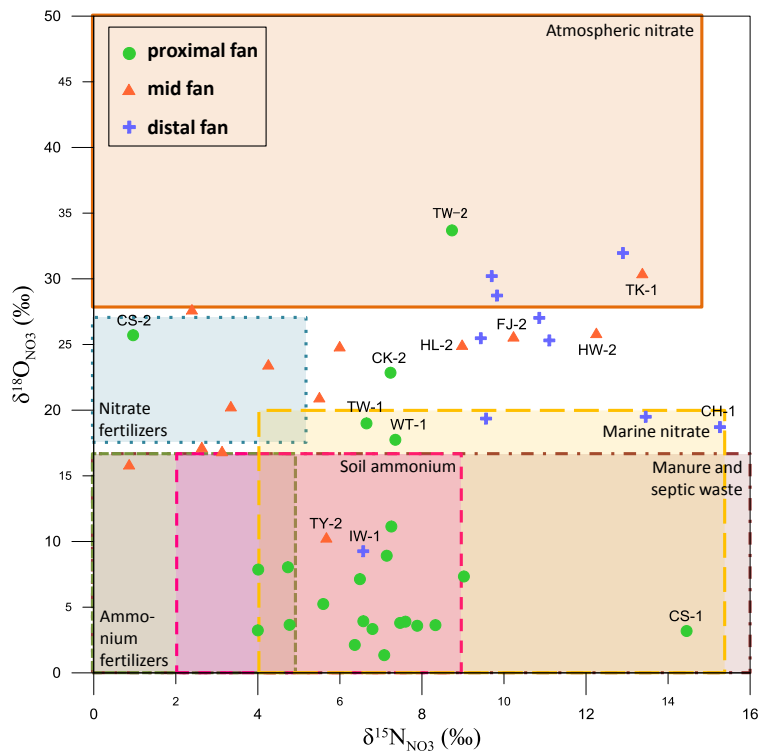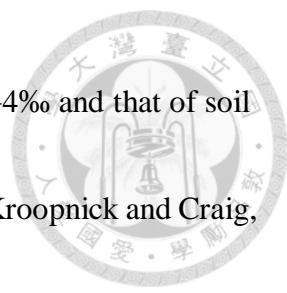

Fig. 11. Schematic for source identification on the basis of $\delta^{15}N_{NO3}$ and $\delta^{18}O_{NO3}$ values obtained for the 46 groundwater samples.

50

5.3.2 Formation and attenuation of NO_3^-

$\delta^{15}N$ in NO_3^- are related to N transformation such as nitrification, assimilation, denitrification, anammox, DNRA and feammox. The $\delta^{15}N$ value of the residual NO_3^- increases exponentially with a decrease in the NO_3^- concentration during denitrification (Clark and Fritz, 1997; Kendall et al., 2007). For example, denitrification of nitrate fertilizers that originally have a distinctive $\delta^{15}N$ value of 0‰ yields residual NO_3^- with a higher $\delta^{15}N$ value in the range of +15‰ to +30‰; this range is similar to that of NO_3^- isotope composition of manure and septic waste (Fig. 3), making it difficult to identify the source (Kendall and Aravena, 2000). However, when NO_3^- is formed by microbial nitrification, it derives two oxygen atoms from oxygen in water molecules and one oxygen atom from DO (Andersson and Hooper, 1983; Hollocher, 1984; Kumar et al., 1983). If there is no fractionation resulting from the incorporation of oxygen from water or O_2, $\delta^{18}O$ of microbial NO_3^- can be regarded as a combination of two oxygen atoms from water and one oxygen atom from O_2 (Eq. (7)). As long as the $\delta^{18}O$ values of water and O_2 are known, this formula can be used to determine whether aerobic nitrification occurs.

$$\delta^{18}O_{NO3} \, (‰) = 2/3 \, \delta^{18}O_{H2O} \, (‰) + 1/3 \, \delta^{18}O_{O2} \, (‰) \tag{7}$$

The $\delta^{18}O_{H2O}$ value of normal water is in the range of −25‰ to +4‰ and that of soil

O_2 is equivalent to that of atmospheric O_2 (approximately +23.5‰) (Kroopnick and Craig,

1972), and therefore, the $\delta^{18}O$ value of soil nitrate formed through in situ nitrification of

NH_4^+ should fall in the range of −8.8‰ to +10.5‰. In Table 2, the average values of

$\delta^{18}O_{NO3}$ in the groundwater of the proximal fan, mid-fan, and distal fan are 9.16‰ ±

8.67‰ (n = 23), 23‰ ± 6.88‰ (n = 13), and 23.57‰ ± 6.85‰ (n = 10), respectively,

indicating that microbial nitrification may occur only in the proximal fan of the Choushui

River alluvial fan; in the current study, the proximal fan was assessed on the basis of the

local DO and ORP values to be in an oxidative state.

N and O isotope compositions are used to determine the causes of NO_3^- attenuation

as well. Denitrification increases the $\delta^{15}N$ and $\delta^{18}O$ values of the residual NO_3^-. Several

studies have shown that the enrichment ratio of N to O associated with denitrification is

close to 1:1 or 2:1 (Fig. 3; Amberger and Schmidt, 1987; Aravena and Robertson, 1998;

Kendall et al., 2007; Mengis et al., 1999; Panno et al., 2006), resulting in $\delta^{15}N_{NO3}$ and

$\delta^{18}O_{NO3}$ increasing in the ratio of approximately 1:1 or 2:1. Fig. 9 clearly shows that

denitrification occurred progressively in the upstream to downstream direction of the

Choushui River. A significant denitrification process appeared at the sampling locations
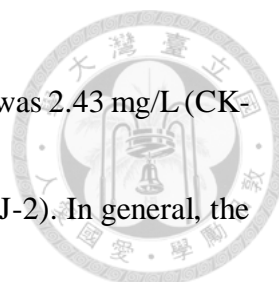
CK-2, HL-2, and FJ-2 sequentially. The initial concentration of NO_3^- was 2.43 mg/L (CK-2) to 0.44 mg/L (HL-2) and the final concentration was 0.09 mg/L (FJ-2). In general, the ideal conditions for the denitrification reaction are as follows: pH = 6.2–10, ORP = −200 to 665 mV, T = 0–50°C, and DO $\leq$ 2 mg/L (Karr et al., 2001); these conditions were present in CK-2, HL-2, and FJ-2.

Kendall (1998) and Mariotti et al. (1988) indicated that the relationship between the NO_3^- concentrations and $\delta^{15}N_{NO3}$ could be formulated as

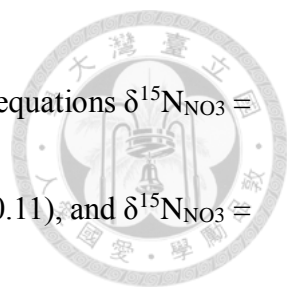$$\delta^{15}N = \delta^{15}N_0 + \varepsilon \ lnNO_3^- \tag{8}$$

because the evolution of the isotope composition of a substrate (residual reactant) during both kinetic and equilibrium processes (isotope fractionation) is generally described by the exponential function of the Rayleigh equation

$$\delta \approx \delta_0 + \varepsilon_{p-s} \ ln(f) \tag{9}$$

where δ_0 is the initial composition of the substrate, f is the remaining fraction of the substrate, and ε_{p-s} is the isotope enrichment factor of the product relative to the substrate. In Eq. (8), the condition $\varepsilon < 0$ (the NO_3^- concentration decreases and ^{15}N increases) supports the assimilation of NO_3^- by living organisms or denitrification of NO_3^- by microorganisms. Fig. 12 presents a plot of $lnNO_3^-$ versus $\delta^{15}N_{NO3}$. The figure indicates

that the relationship between $\ln NO_3^-$ and $\delta^{15}N_{NO3}$ corresponds to the equations $\delta^{15}N_{NO3} = 6.48 + 0.17 \ln NO_3^-$ ($R^2 = 0.28$), $\delta^{15}N_{NO3} = 4.81 - 1.07 \ln NO_3^-$ ($R^2 = 0.11$), and $\delta^{15}N_{NO3} = 10.36 - 0.32 \ln NO_3^-$ ($R^2 = 0.13$) for the proximal fan, mid-fan, and distal fan, respectively.

Therefore, assimilation or denitrification is likely to occur in the groundwater of the mid-fan ($\varepsilon = -1.07$) and distal fan ($\varepsilon = -0.32$) of the Choushui River alluvial fan, leading to relatively low NO_3^- concentrations. By contrast, the groundwater of the proximal fan ($\varepsilon = 0.17$) is not favorable for promoting these reactions. Aravena and Robertson (1998) found that denitrification causes ε to lie in the range of $-40‰$ to $-5‰$, Fukada et al. (2003, 2004) suggested that the ε value should fall to $-13.6‰$ if denitrification occurs, and Seiler (2005) observed the ε value to be $-5.7‰$ during denitrification. The aforementioned researches indicated that there is no strong evidence for the occurrence of a significant denitrification process in the Choushui River alluvial fan. By contrast, the ε value falls in the range of $-30‰$ to $0‰$ if NO_3^- is assimilated into living organisms such as plants (Cifuentes et al., 1989; Kendall et al., 2007; Montoya et al., 1991), indicating that assimilation occurs and might be a dominant process in the groundwater of the mid-fan and the distal fan of the Choushui River alluvial fan.

By using different versions of the scaled tube and pyrolysis methods, many studies
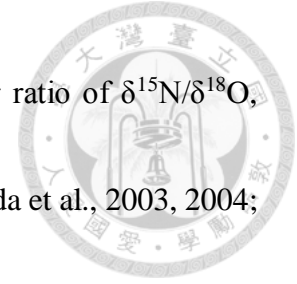
have established that the denitrification of NO_3^- results in a linear ratio of $\delta^{15}N/\delta^{18}O$,

which lies in the range 1.3–2.1 (Aravena and Robertson, 1998; Fukada et al., 2003, 2004;

Mengis et al., 1999; Panno et al., 2006). Fig. 9 shows the equations describing the

relationship between $\delta^{15}N_{NO3}$ and $\delta^{18}O_{NO3}$ in the groundwater samples of the proximal

fan, mid-fan, and distal fan of the Choushui River alluvial fan; the equations for these

three fan regions are $\delta^{18}O_{NO3} = -0.53\ \delta^{15}N_{NO3} + 12.75$ ($R^2 = 0.22$), $\delta^{18}O_{NO3} = 0.84\ \delta^{15}N_{NO3}$

$+ 16.83$ ($R^2 = 0.35$), and $\delta^{18}O_{NO3} = 0.67\ \delta^{15}N_{NO3} + 16.29$ ($R^2 = 0.58$), respectively. The

ratio $\delta^{15}N/\delta^{18}O$ was calculated for the proximal fan, mid-fan, and distal fan, and the values

obtained were -1.89, 1.19, and 1.49, respectively. Only the ratio for the distal fan was in

the range 1.3–2.1, which warrants the occurrence of NO_3^- denitrification. The ratio for

the mid-fan suggests that NO_3^- denitrification was insignificant.

In summary, the groundwater in the proximal fan shows no signs of NO_3^-

assimilation or denitrification reactions but reveals microbial nitrification, which leads to

relatively high NO_3^- concentrations. The groundwater in the mid-fan shows signs of NO_3^-

assimilation and insignificant denitrification; hence, the depletion of NO_3^- might be

dominated by assimilation to a certain extent. The groundwater in the distal fan strongly

shows signs of NO_3^- denitrification, which results in relatively low NO_3^- concentrations,

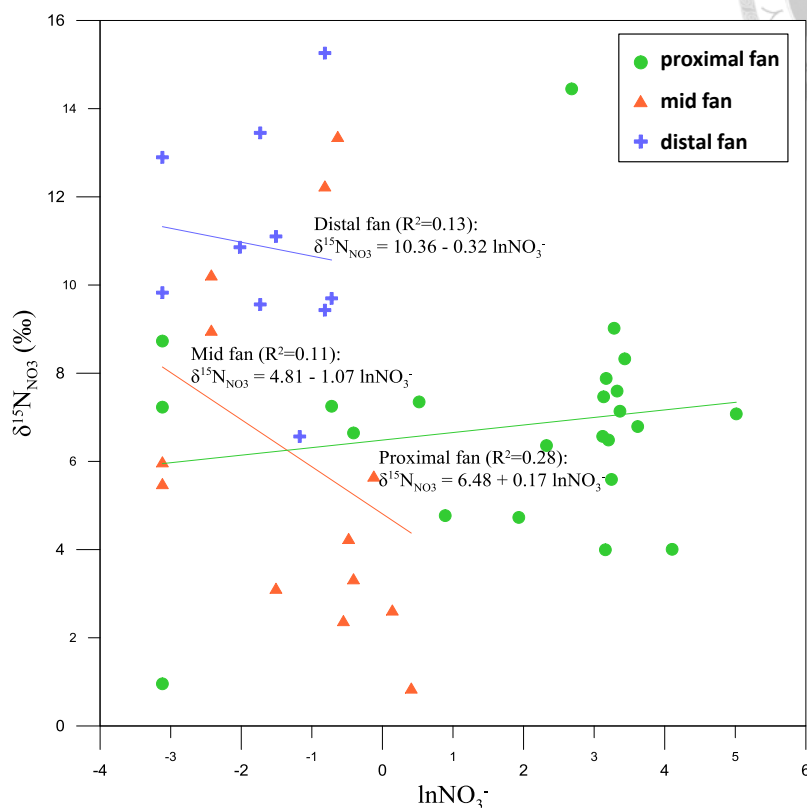and assimilation might occur simultaneously with denitrification in this region.
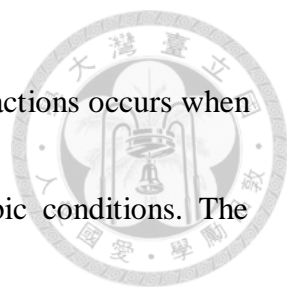
Fig. 12. Formulated relationship between $\delta^{15}N_{NO3}$ and $lnNO_3^-$ for the 46 groundwater samples.

5.4 As mobility in the N-budget system

Fig. 13 indicates that high concentrations of As appeared in relatively high $\delta^{15}N_{NO3}$ values in the distal fan and relatively low $\delta^{15}N_{NO3}$ values in the mid-fan, which may be governed by denitrification and feammox processes, respectively. Denitrification elevates the values of $\delta^{15}N_{NO3}$ in NO_3^-, whereas feammox lowers them. The released As to groundwater is associated with reactions of Fe oxyhydroxides in both the high and the low values of $\delta^{15}N_{NO3}$ environment.

56

Smedley et al. (2002) suggested that a sequence of reduction reactions occurs when conditions in aquifers change from aerobic conditions to anaerobic conditions. The change begins from the microbial decomposition of organic matter, and simultaneously, O_2 (DO) is consumed and dissolved CO_2 in the groundwater increases. Subsequently, NO_3^- decreases because of its reduction to NO_2^-, N_2O, and N_2 (denitrification). Insoluble manganic oxides dissolve and are reduced to soluble Mn^{2+}, and hydrous ferric oxides (often Fe^{3+} compounds) are reduced to Fe^{2+}. This reduction to Fe^{2+} is followed by the reduction of SO_4^{2-} to S^{2-}, fermentation, and methanogenesis, resulting in the formation of CH_4^-. Finally, N_2 is reduced to NH_4^+. The reduction of As^{5+} to As^{3+} often occurs after the reduction of Fe^{3+} and before the reduction of SO_4^{2-}. Because the most possible hypothesis of As release mechanisms is the reduction of Fe oxyhydroxides (Nickson et al., 2000; Harvey et al., 2002; Lu et al., 2010), the processes influencing Fe redox reactions are crucial.

The enrichment of both As and NH_4^+ in groundwater may be attributed to the high concentration of N and the consumption of O_2 by microorganisms. The reductive environment further enhances the reductive dissolution of As-bearing Fe oxyhydroxides and the desorption of adsorbed As, resulting in the release of As into groundwater (Xiong

57

et al., 2015).

Furthermore, the presence of NO_3^- has a deciding influence on the redox environment, which directly affects the mobility of As (Harvey et al., 2002; Mayorga et al., 2013). High NO_3^- concentrations in the groundwater of the proximal fan may not be favorable for the dissolution of As-containing Fe oxyhydroxides. However, after the reduction of NO_3^- and the dissolution of As-containing Fe oxyhydroxides, As^{5+} is sequentially reduced to As^{3+} in the groundwater of the mid-fan and the distal fan. The distinct denitrification process lowers the ORP, creating an anaerobic environment and promoting the reductive dissolution of As-containing Fe oxyhydroxides; the reductive dissolution leads to the release of As into the groundwater.

In the mid-fan and the distal fan, the reductive dissolution of Fe oxyhydroxides and the auxiliary denitrification process are suggested to be the main processes responsible for As release into the groundwater. Hsu et al. (2010) used factor analysis to identify factors that govern the chemistry of As-affected groundwater, and the results suggested that the reductive dissolution of Fe oxyhydroxides occurred in the high NH_4^+ concentration area in the distal fan of the Choushui River alluvial fan. According to the statistical analysis results, Hsu et al. (2010) estimated that the denitrification processes
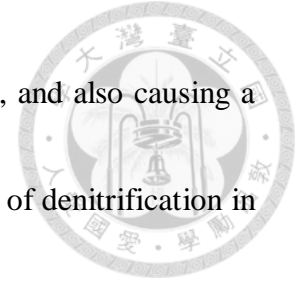
58

might lower the redox potential, creating an anaerobic environment, and also causing a reductive release of As to groundwater. In this study, the occurrence of denitrification in the distal fan supports their results.

Furthermore, feammox process may influence $\delta^{15}N$ values in NO_3^-. An anaerobic reaction termed feammox is the reduction of Fe^{3+} being coupled to NH_4^+ oxidation through Eq. (10) (Yang et. al, 2012; Zhang et. al, 2014).

$$3Fe(OH)_3+5H^++NH_4^+\rightarrow3Fe^{2+}+9H_2O+0.5N_2 \qquad (10)$$
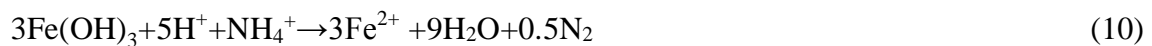
Yang et al. (2012) used labeled Fe_3^+ and NH_4^+ to assess the presence of feammox. However, the importance of feammox remains unknown because microcosm experiments have not been executed. Given the complexity of N cycling, feammox remains a potential reaction that needs to be further studied (Tekin, 2012). Feammox to N_2 is energetically favorable over a wide range of conditions including pH range. Table 3 and 4 show the concentrations of As, NH_4^+ and Fe (especially Fe_2^+) were relatively high in the mid-fan and the distal fan, and Table 5 shows the relations between As, NH_4^+ and Fe were statistically significant, reaching moderate-to-high positive correlations, both interpreting a likely environment and enough concentrations for the occurrence of anaerobic reaction of feammox. According to Eq. (10), when Fe oxyhydroxides are reduced by NH_4^+, the

59

desorption of adsorbed As from Fe oxyhydroxides may occur, resulting in an enriched As

and Fe^{2+} environment.

In conclusion, the denitrification and the feammox are two main processes responsible for the release of As into the groundwater in the Choushui River alluvial fan. However, the contribution of denitrification and feammox to As release needs to be further quantified because some chemical reactions without presence of N compound, such as anaerobic organic matter degradation and anaerobic methane oxidation, may also contribute to Fe^{3+} reduction, and indirectly influence the release of As.

Table 6 shows the summary of dominant N sources, N compounds and N redox reactions in the Choushui River alluvial fan. Fig. 14 presents a site conceptual model (SCM) of the sources and transformation of N-containing contaminants in the As-contaminated groundwater of the Choushui River alluvial fan.
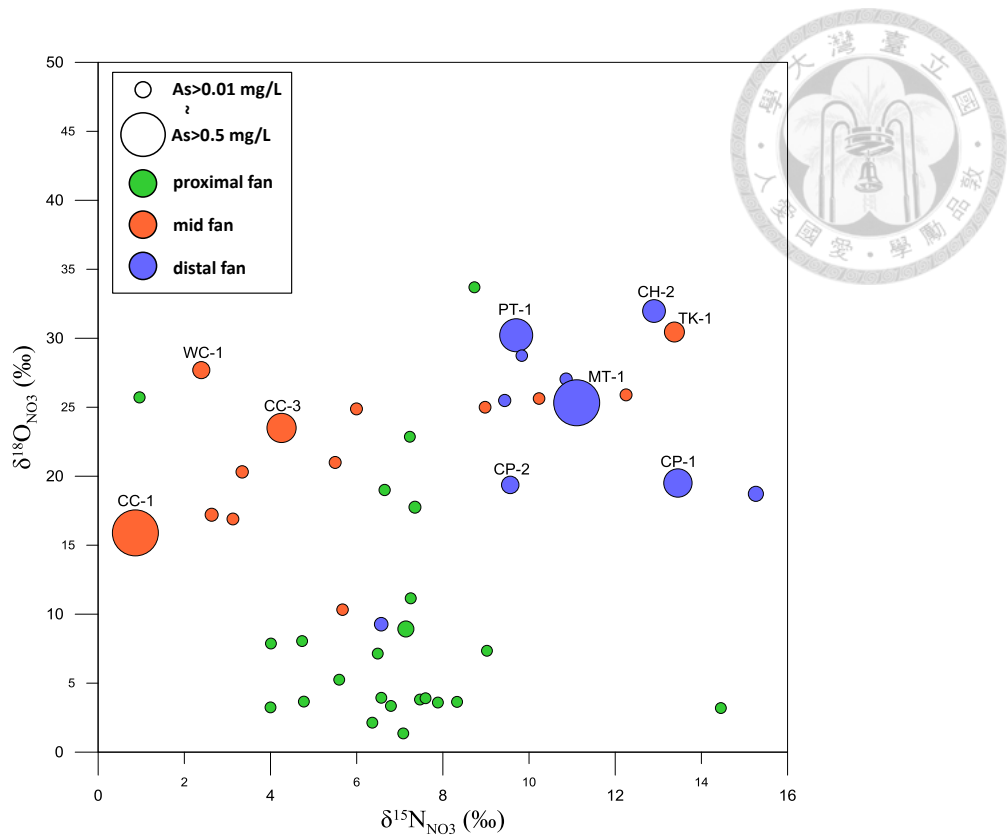
Fig. 13. Plot of As concentration on $\delta^{15}N_{NO3}$ versus $\delta^{18}O_{NO3}$ diagram for the 46 groundwater samples.

Table 6. Dominant N sources, N compounds and N redox reactions in the Choushui River alluvial fan.

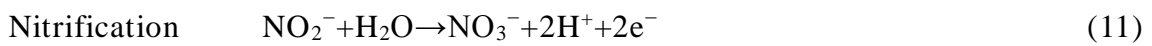| Fan region	distal fan	mid-fan	proximal fan
Redox status	more anaerobic	facultative	more aerobic
Dominant N sources	nitrate fertilizers and marine nitrate	nitrate fertilizers and marine nitrate	ammonium fertilizers, manure and septic waste
Dominant N redox reactions	• NO_3^- reduction • Mn & Fe oxyhydroxides dissolve to Mn^{2+} & Fe^{2+} • reduction of As^{5+} to As^{3+}	• feammox • DO consumption • NO_3^- reduction • Mn & Fe oxyhydroxides dissolve to Mn^{2+} & Fe^{2+}	oxidation of NH_4^+
Dominant N compounds	abundant NH_4^+	$NH_4^+ > NO_3^-$	abundant NO_3^-
Abundance of $^{15}N_{NO3}$ and $^{18}O_{NO3}$	enrichment of $^{15}N_{NO3}$ and $^{18}O_{NO3}$ (influenced by denitrification)	depletion of $^{15}N_{NO3}$ (influenced by feammox)	depletion of $^{18}O_{NO3}$ (influenced by atmospheric O_2)
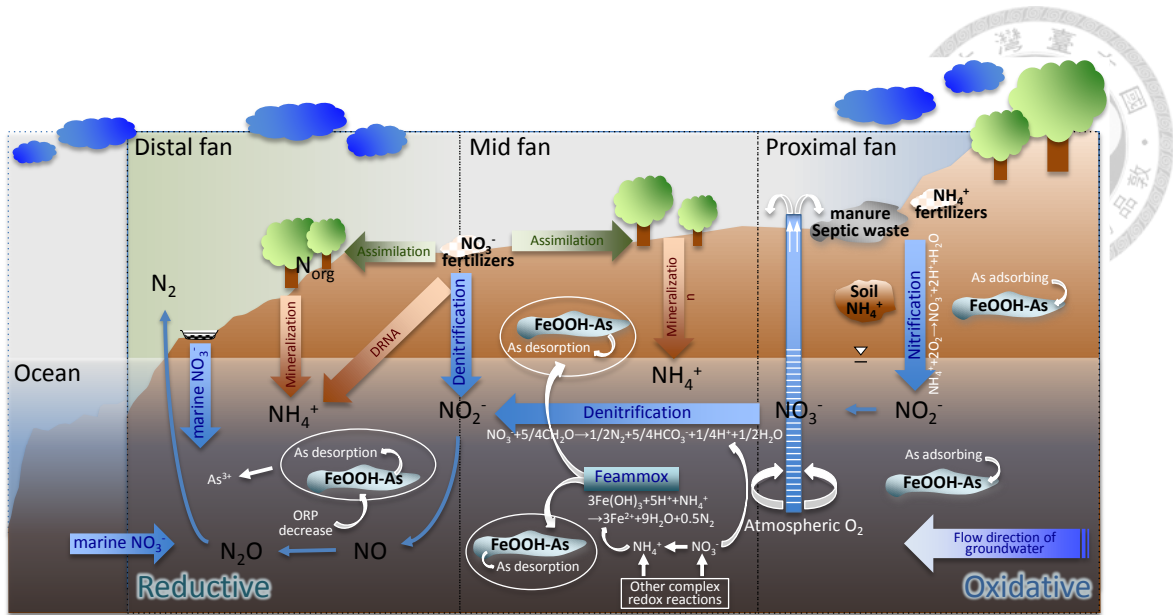
Fig. 14. The SCM of the sources and transformation of N-containing contaminants in the arsenic contaminated groundwater of the Choushui River alluvial fan.
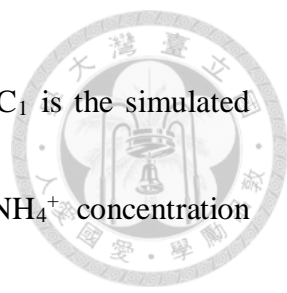
5.5 The PHREEQC simulations of N cycling in As-rich groundwater

5.5.1 The NH_4^+ concentration differences after nitrification simulation

In the database (Amm.dat) of PHREEQC, the oxidative reactions of N cycling include nitrification (Eq. (11)) and feammox (Eq. (12)). Nitrification is the biological oxidation of NH_3 or NH_4^+ to NO_2^- followed by the oxidation of NO_2^- to NO_3^-. Feammox is an anaerobic reduction consuming NH_4^+ and producing NO_3^-, NO_2^-, or N_2.

Nitrification $\qquad NO_2^- + H_2O \rightarrow NO_3^- + 2H^+ + 2e^-$ (11)

Feammox $\qquad NH_4^+ + 3H_2O \rightarrow NO_3^- + 10H^+ + 8e^-$ (12)

The simulation result of NH_4^+ concentrations after nitrification in the 37 samples was summarized in Table 7. NH_4^+ concentration differences represent $(C_1 - C_0)/C_0 \times 100$ (%),

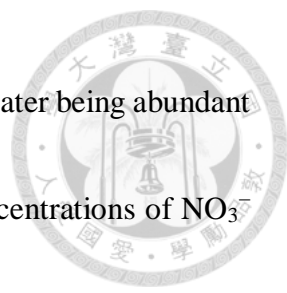where C_o is the analyzed concentration (mg/L) by laboratory and C_1 is the simulated concentration (mg/L) by PHREEQC. The mean values of the NH_4^+ concentration differences in the groundwater of the proximal fan, mid-fan, and distal fan are -92.31% $\pm 12.67\%$ ($n = 15$), $-69.70\% \pm 21.17\%$ ($n = 12$), and $-14.70\% \pm 14.82\%$ ($n = 10$), respectively (Table 7). In other words, 92.31% of NH_4^+ in the proximal fan, 69.70% of NH_4^+ in the mid-fan, and 21.17% of NH_4^+ in the distal fan simulatively oxidized to NO_3^- through nitrification and/or feammox. These data clearly show that the nitrification and/or feammox mostly occur in the proximal fan and mid-fan, whereas they slightly occur in the distal fan.

An anaerobic reaction termed feammox is the reduction of Fe^{3+} being coupled to NH_4^+ oxidation. It consumes NH_4^+ and produces NO_3^-, NO_2^-, or N_2 (Yang et. al, 2012; Zhang et. al, 2014). Further, feammox may lower $\delta^{15}N$ values in NO_3^-. When Fe oxyhydroxides are reduced by NH_4^+, the desorption of adsorbed As from Fe oxyhydroxides may occur, resulting in an enriched As and Fe^{2+} environment (Yang et al., 2012). Weng et al. (2017) reported that high concentrations of As, NH_4^+ and Fe and depletion of $\delta^{15}N_{NO3}$ imply the occurrence of feammox process in the mid-fan of the Choushui River alluvial fan, verifying the inference of this study.

The reaction of nitrification leads to the consequence of groundwater being abundant in NO_3^- and depleted in NH_4^+ (Fig. 2). Table 3 shows the mean concentrations of NO_3^- and NH_4^+ in the proximal fan are 23.62 mg/L and 0.17 mg/L, respectively, evidently supporting the occurrence of NH_4^+ nitrification. Liu et al. (2006) suggested that high NO_3^- concentrations were found in the oxidative proximal fan, whereas low NO_3^- concentrations were observed in the reductive distal fan. Moreover, Weng et al. (2017) used $\delta^{15}N_{NO3}$ and $\delta^{18}O_{NO3}$ to identify the occurrence of nitrification, and indicated that microbial nitrification occurred in the proximal fan of the Choushui River alluvial fan. In this study, the proximal fan was assessed on the basis of local DO and ORP values to be in an oxidative state, initiatively urging the occurrence of nitrification.

Table 7. Detailed NH_4^+ simulation results of nitrification in the groundwater samples obtained from the Choushui River alluvial fan.

Proximal fan (15 wells)		Mid fan (12 wells)		Distal fan (10 wells)	
Wells	NH_4^+ concentration difference (%)	Wells	NH_4^+ concentration difference (%)	Wells	NH_4^+ concentration difference (%)
CK-1	−99.96	CC-1	−77.43	CH-1	−6.92
CK-2	−72.74	CC-3	−34.58	CH-2	−26.34
CS-2	−63.80	FJ-2	−41.92	CP-1	−1.86
HK-2	−95.91	HC-1	−87.82	CP-2	−8.20
KK-1	−97.25	HH-1	−65.69	HY-2	−13.52
LH-1	−99.42	HL-2	−65.16	IW-1	−37.35
NT-2	−99.90	HW-2	−71.91	IW-3	−41.27
SH-1	−97.56	TK-1	−56.60	IW-4	−4.37
TC-1	−99.77	WC-1	−85.11	MT-1	−4.18
TH-1	−98.39	WC-2	−51.55	PT-1	−3.04
TH-2	−99.55	WC-3	−99.50		
TW-1	−99.17	WC-4	−99.15		
TW-2	−68.01				
WT-1	−96.88				
WT-2	−96.31				
Mean	*−92.31*	*Mean*	*−69.70*	*Mean*	*−14.70*
SD	*12.67*	*SD*	*21.17*	*SD*	*14.82*

Table 7 shows the detailed results of nitrification simulation, including the NH_4^+ concentration differences in each well and the standard deviation (SD) of concentration differences in each fan. The simulated NH_4^+ speciation results suggest that the values of NH_4^+ concentration differences in the groundwater of the proximal fan, mid-fan, and distal fan range from −63.80% to −99.96%, −34.58% to −99.50%, and −1.86% to

−41.27% (Table 7), respectively. The most depletion of NH_4^+ (the highest negative value) was observed in the well of CK-1, which is located in the proximal fan, indicating that the nitrification reaction occurs energetically. The least depletion of NH_4^+ (the lowest negative value) was observed in the well of CP-1, which is located in the distal fan and accompanied with high concentrations of TOC and NH_4^+ (Table 3), supporting the consequence of less reaction of nitrification.

The NH_4^+ concentration differences of 12 sampling wells among 15 sampling wells in the proximal fan are greater than 95% (Table 7). The most depletion of NH_4^+ was observed in CK-1, reaching −99.96%, followed by NT-2 with −99.90%. The sampling wells of CK-1 and NT-2 have depths of 59 m and 96 m, and DO of 0.17 mg/L and 4.69 mg/L (Table 3), respectively, indicating a relatively shallow and oxidative condition in groundwater, and therefore, providing a favorable environment for triggering the reaction of nitrification.
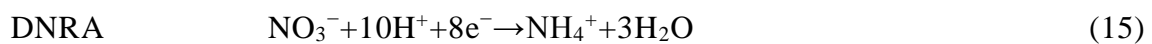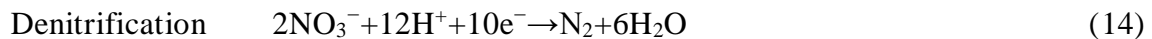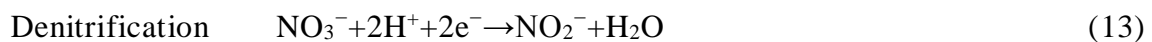
On the contrary, CS-2 with the least depletion of NH_4^+ of −63.80% and TW-2 with the second least of −68.01% in the proximal fan may be related to deeper well depths (199.3 m and 244 m, respectively) and low DO (both are 0.01 mg/L), suggesting that a relatively reductive state refrains from nitrification.
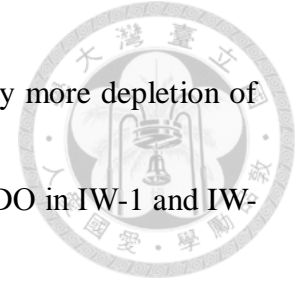
In the distal fan, the wells of IW-1 and IW-3 have the relatively more depletion of

NH_4^+, reaching −37.35% and −41.27%, respectively. The values of DO in IW-1 and IW-

3 reach 0.09 and 0.15 mg/L (Table 3), and the other physicochemical parameters of EC,

Cl^-, and SO_4^{2-} also show the influence of seawater infiltration or intrusion, which may

enhance the occurrence of nitrification in the groundwater.

5.5.2 The NO_3^- concentration differences after denitrification simulation

In the database (Phreeqc.dat) of PHREEQC, the reductive reactions of N cycling

include denitrification (Eq. (13) and (14)) and dissimilatory NO_3^- reduction to NH_4^+

(DNRA) (Eq. (15)). Denitrification is the sequential reduction of NO_3^- to gaseous

products ($NO_3^- \rightarrow NO_2^- \rightarrow NO \rightarrow N_2O \rightarrow N_2$). DNRA is defined as anaerobic

reduction of NO_3^- to NH_4^+ by microbes.

Denitrification $\quad NO_3^- + 2H^+ + 2e^- \rightarrow NO_2^- + H_2O$ (13)

Denitrification $\quad 2NO_3^- + 12H^+ + 10e^- \rightarrow N_2 + 6H_2O$ (14)

DNRA $\quad NO_3^- + 10H^+ + 8e^- \rightarrow NH_4^+ + 3H_2O$ (15)

The simulation result of NO_3^- concentrations after denitrification in the 18 samples

was summarized in Table 8. The mean values of the NO_3^- concentration differences in

the groundwater of the mid-fan and distal fan are −32.93% ±20.60% ($n = 5$) and −61.13%

67

± 27.92 ($n = 9$), respectively (Table 8). In other words, 32.93% of NO_3^- in the mid-fan

and 61.13% of NO_3^- in the distal fan simulatively reduced to N_2 or NH_4^+ through
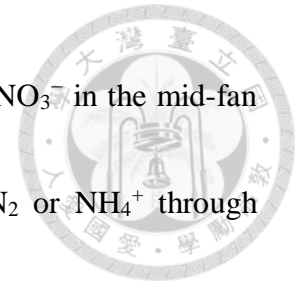
denitrification and/or DNRA.

Table 8. Summary of NO_3^- and As simulation results of denitrification in the groundwater samples obtained from the Choushui River alluvial fan.

Fan area	Number of wells	Average NO_3^- concentration difference (%)	SD (%)	Average As concentration difference (mg/L)
Proximal fan	4	-	-	As^{3+} : $-1.32E-4$ (As^{5+} : $+1.32E-4$)
Mid fan	5	-32.93	20.60	As^{3+} : $+6.62E-3$ (As^{5+} : $-6.62E-3$)
Distal fan	9	-61.13	27.92	As^{3+} : $+6.40E-3$ (As^{5+} : $-6.40E-3$)

Table 3 shows the mean concentrations of NO_3^- in the proximal fan, the mid-fan, and the distal fan are 23.62 mg/L, 0.53 mg/L, and 0.25 mg/L, respectively. The spatial concentration distribution of NO_3^- from the proximal fan to the distal fan indicates the gradual occurrence of NO_3^- denitrification and/or DNRA from upstream to downstream of the Choushui River alluvial fan. In this study, the mid-fan and the distal fan were assessed on the basis of the local DO and ORP values to be in relatively more reductive conditions, driving the occurrence of denitrification and/or DNRA.
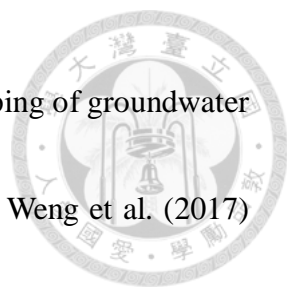
Furthermore, the mean concentration of NH_4^+ in the distal fan reaches 6.69 mg/L (Table 3), indicating that in addition to denitrification, DNRA might be the dominant process of N cycling in the distal fan (Fig. 2, Eq. (15)). Weng et al. (2017) suggested that assimilation, mineralization, DNRA, and denitrification should occur simultaneously in the distal fan of the Choushui River alluvial fan, resulting in the depletion of NO_3^- and

69

enrichment of NH_4^+ in the groundwater.

Table 8 also shows the simulated As speciation results. In the proximal fan, As^{3+} decreased by 1.32E−4 mg/L (As^{5+} increased by 1.32E−4 mg/L), and this valence transformation of As species and As concentration difference seem comprehensible because the on-site condition of the proximal fan is under oxidative condition. As^{3+} theoretically oxidizes to As^{5+} in oxidative state. By contraries, in the mid-fan and the distal fan, the reductive state was observed base on the DO and ORP data of the groundwater (Table 3), and the circumstance of reduction from As^{5+} to As^{3+} was obvious in Table 8, reaching 6.62E−3 mg/L and 6.40E−3 mg/L, respectively. Hsu et al. (2010) estimated that the denitrification processes might lower the redox potential, creating an anaerobic environment, and also causing a reductive release of As to groundwater.

Table 9 shows the detailed results of denitrification simulation. The slight and less NO_3^- denitrification reaction in the mid-fan occurs in the well of TK-1, and that of in the distal fan occurs in the well of PT-1, followed by CH-1. By reviewing the physicochemical characteristics of groundwater in Table 3, high EC(~21,750 μmho/cm), Cl^- (~7,470 mg/L), and SO_4^{2-} (~1,150 mg/L) were found in the aforementioned wells, and these observations indicate that TK-1, PT-1, and CH-1 are influenced by seawater

infiltration or intrusion causing by aquaculture activity and overpumping of groundwater or by the existence of paleo-marine environment (Kao et al., 2011). Weng et al. (2017) also evidenced that CH-1 with the highest δD_{H2O} and $\delta^{18}O_{H2O}$ values attributed to seawater infiltration or intrusion and paleo-marine environment, being the main cause of offset between the meteoric water lines. Therefore, the infiltration or intrusion and paleo-marine environment may result in the inhibition of denitrification reaction in TK-1 in the mid-fan and PT-1 and CH-1 in the distal fan.

By contrast, the most intense NO_3^- denitrification reaction in the mid-fan occurs in the well of CC-3, and that of in the distal fan occurs in the wells of CH-2 and CP-2, followed by IW-3. The wells of CC-3, CH-2, CP-2, and IW-3 have the depths of 111.5 m, 147.42 m, 173.8 m, and 219 m (Table 3), respectively, suggesting that the occurrence of denitrification is mostly in deep wells, which are observed to be more reductive than the shallow wells on the basis of the DO and ORP analyzed data of the groundwater.

Table 9. Detailed NO_3^- simulation results of denitrification in the groundwater samples obtained from the Choushui River alluvial fan.

Mid fan (5 wells)		Distal fan (9 wells)	
Wells	NO_3^- concentration difference (%)	Wells	NO_3^- Concentration difference (%)
CC-1	−32.98	CH-1	−32.80
CC-3	−57.79	CH-2	−100.00
HH-1	−15.95	CP-1	−50.26
TK-1	−6.92	CP-2	−100.00
WC-1	−51.03	HY-2	−46.44
		IW-1	−76.20
		IW-3	−82.13
		MT-1	−32.98
		PT-1	−29.35
Mean	*−32.93*	*Mean*	*−61.13*
SD	*20.60*	*SD*	*27.92*

5.5.3 The discrepancy of $\delta^{15}N_{NO3}$ after denitrification simulation

The values of $\delta^{15}N$ in NO_3^- are related to N transformation such as nitrification, assimilation, denitrification, anammox, DNRA and feammox. Clark and Fritz (1997) and Kendall et al. (2007) suggested that the $\delta^{15}N$ value of the residual NO_3^- increases with a decrease in the NO_3^- concentration during denitrification.

The discrepancy of $\delta^{15}N$ in NO_3^- in groundwater was simulated on the basis of the influence of the reaction of NO_3^- denitrification. The isotope differences represent $(\delta^{15}N_1 - \delta^{15}N_0)/ \delta^{15}N_0 \times 100$ (%) in NO_3^-, where $\delta^{15}N_0$ is the analyzed isotope value (‰) by laboratory and $\delta^{15}N_1$ is the simulated isotope value (‰) by PHREEQC. Table 10

72

doi:10.6342/NTU201900143

indicates that the values of $\delta^{15}N_{NO3}$ in the groundwater of the mid-fan and the distal fan increased by +2.11% and +5.79%, with the SD of 1.42% ($n = 3$) and 5.83% ($n = 7$), respectively.
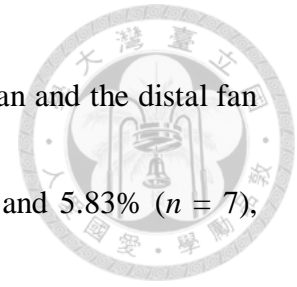
Karr et al. (2001) indicated that denitrification increases $\delta^{15}N$ values of the residual NO_3^-, and the ideal conditions for the denitrification reaction are as follows: pH = 6.2 to 10, ORP = −200 to 665 mV, T = 0 to 50°C, and DO ≤ 2 mg/L; these conditions were present in most wells in the distal fan, and partial wells in the mid-fan of the Choushui River alluvial fan. The reductive environment further enhances the reductive dissolution of As-bearing Fe oxyhydroxides and the desorption of adsorbed As, resulting in the release of As into groundwater (Xiong et al., 2015). Also, Weng et al. (2017) suggested that the process of NO_3^- denitrification resulted in the enrichment of NO_3^- in the distal fan, and the denitrification occurred in the mid-fan as well.

Table 10. Detailed $\delta^{15}N_{NO3}$ simulation results of denitrification in the groundwater samples obtained from the Choushui River alluvial fan in 2015.

Mid fan (3 wells)		Distal fan (7 wells)	
Wells	$\delta^{15}N_{NO3}$ difference (%)	Wells	$\delta^{15}N_{NO3}$ difference (%)
CC-1	+1.81	CH-1	+1.74
HH-1	+0.69	CP-1	+3.68
WC-1	+3.83	HY-2	+3.17
		IW-1	+11.77
		IW-3	+16.87
		MT-1	+1.78
		PT-1	+1.50
Mean	*+2.11*	*Mean*	*+5.79*
SD	*1.42*	*SD*	*5.83*

Moreover, Table 10 shows that the increased values of $\delta^{15}N_{NO3}$ range from +0.69% (HH-1) to +3.83% (WC-1) in the mid-fan. All values of $\delta^{15}N_{NO3}$ difference are <5%, suggesting that the denitrification in the mid-fan occurs but the extent may be slight. Compared with the $\delta^{15}N_{NO3}$ differences in the distal fan, the obviously increased $\delta^{15}N_{NO3}$ values represented in the wells of IW-3 and IW-1, both reaching > 10%; this suggests that the progressive NO_3^- denitrification gave a specific impact to the values of $\delta^{15}N_{NO3}$ in the distal fan.

Table 10 also shows that IW-3 had the highest $\delta^{15}N_{NO3}$ difference, reaching +16.87%, while IW-1 had the second highest $\delta^{15}N_{NO3}$ difference, reaching +11.77%. Both IW-3 and IW-1 have high NO_3^- concentration differences after denitrification, reaching −82.13%

and −76.20% (Table 9), respectively, and this suggests that the denitrification occurred in the distal fan certainly resulted in the enrichment of $\delta^{15}N_{NO3}$ in groundwater.

Nevertheless, the increased values of $\delta^{15}N_{NO3}$ range from +1.50% (PT-1) to +16.87% (IW-3) in the distal fan. Among these 7 wells, PT-1 has the lowest $\delta^{15}N_{NO3}$ difference. Table 9 shows that the less NO_3^- denitrification reaction in the distal fan occurs in the well of PT-1, being −29.35%, supporting the slight difference of $\delta^{15}N_{NO3}$ in PT-1.

5.5.4 The 1-D transport of N compounds in As-rich groundwater

Fig. 15 shows the spatial divisions of 1-D transport, including the proximal fan, the mid-fan, and the distal fan. The groundwater physicochemical characteristics of well NT-2, WT-1, and HY-2 represent the areas of the proximal fan, the mid-fan, and the distal fan, respectively.

Fig. 16 shows the 1-D transport simulation result of different groundwater parameters from the aforesaid representative sampling wells. The transport result of NO_3^- suggested that denitrification and/or assimilation occur from the mid-fan of the Choushui River Alluvial Fan to the distal fan (Fig. 16a). Weng et al. (2017) suggested that the NO_3^- assimilation is the dominant response to NO_3^- attenuation in the mid-fan, and denitrification is insignificant. Fig. 16b also indicates that nitrification and/or feammox

75

is observed at the beginning of the proximal fan. However, the low concentrations of Fe^{2+}

in the proximal fan imply the occurrence probability of feammox is slim (Eq. (10) and

Table 3).
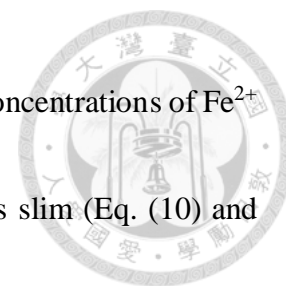
The formation and transportation of NH_4^+ occur only in the distal fan, which may

attribute to the reactions of mineralization form organic N compounds, DNRA from NO_3^-,

and/or N-fixation from N_2. The reductive environment further keeps N compounds to

remain on NH_4^+ formation. The initial and twenty-five years of NO_3^- and NH_4^+ transport

have little shift backward but are insignificant.

The total amount of As increased along the upstream to the downstream of the

Choushui River (Fig. 16c). The concentration of As^{5+} increased at the beginning of the

mid-fan (Fig. 16d), which may be caused by the reductive dissolution of As-bearing Fe

oxyhydroxides and the desorption of adsorbed As, resulting in increase in As in

groundwater. The concentration of As^{3+} increased obviously at the beginning of the distal

fan (Fig. 16e), which may be related to the transformation of As^{5+} to As^{3+} in the reductive

environment, and the continuous desorption of As from Fe oxyhydroxides simultaneously.

The concentration analysis of on-site groundwater samples shows the gradual increase in

As from the proximal fan to the distal fan, verifying the aforesaid simulation result (Table

76

3).

Both the concentrations of Fe^{3+} and Fe^{2+} increased at the end of proximal, causing by the reductive dissolution of Fe oxyhydroxides. The transformation of Fe^{3+} to Fe^{2+} occurred soon when the groundwater reached the mid-fan (Fig. 16f and 16g), resulting in depletion of Fe^{3+} and increase in Fe^{2+} in groundwater. The increase in Fe^{2+} is not only related to the reductive environment, but also attributed to the reaction of feammox (Eq. (10)), which Fe oxyhydroxides react with NH_4^+ and produce Fe^{2+} in the groundwater. Weng et al. (2017) indicated that high concentrations of As, NH_4^+, and Fe and the depletion of $\delta^{15}N_{NO3}$ imply the occurrence of feammox process in the mid-fan of the Choushui River Alluvial Fan.
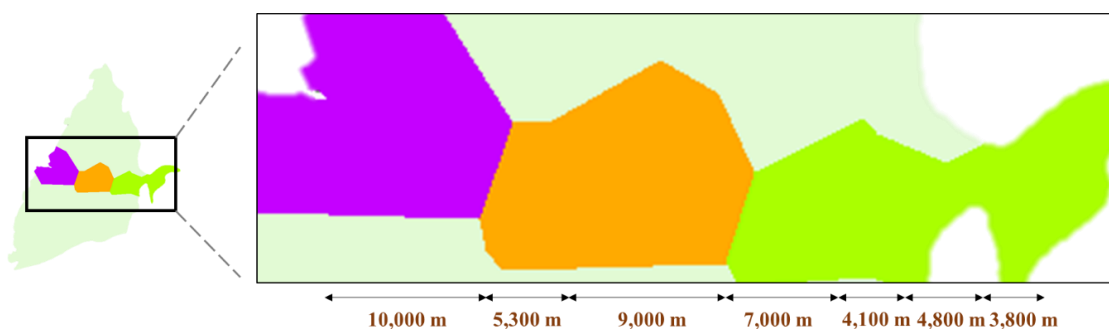

Fig. 15. The spatial divisions of 1-D transport in PHREEQC. ▣: proximal fan; ▣: mid fan; ▣: distal fan.
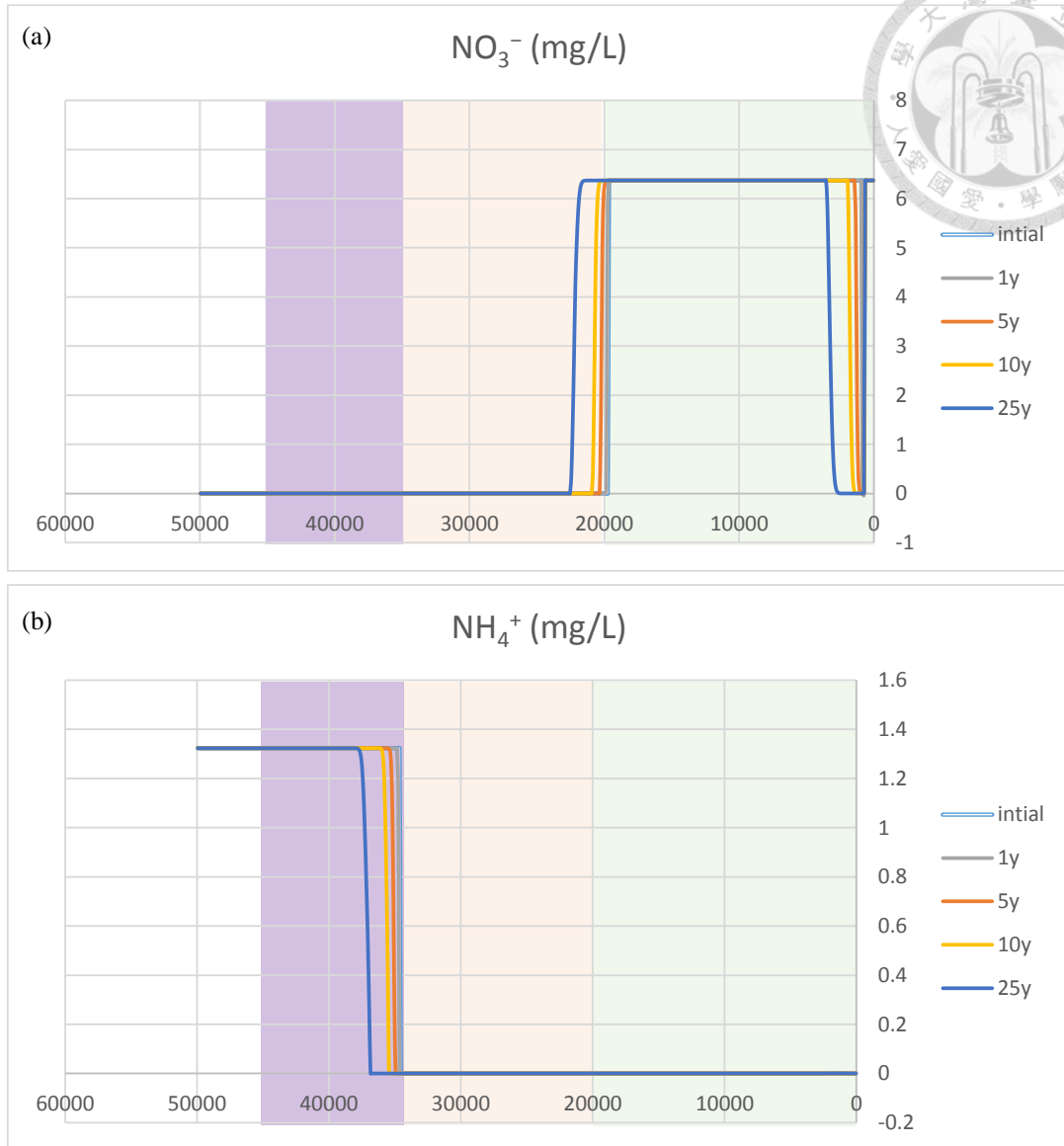
77

Fig. 16. 1-D transport simulation result of different groundwater parameters from the representative groundwater samples. □: proximal fan; □: mid fan; □: distal fan.
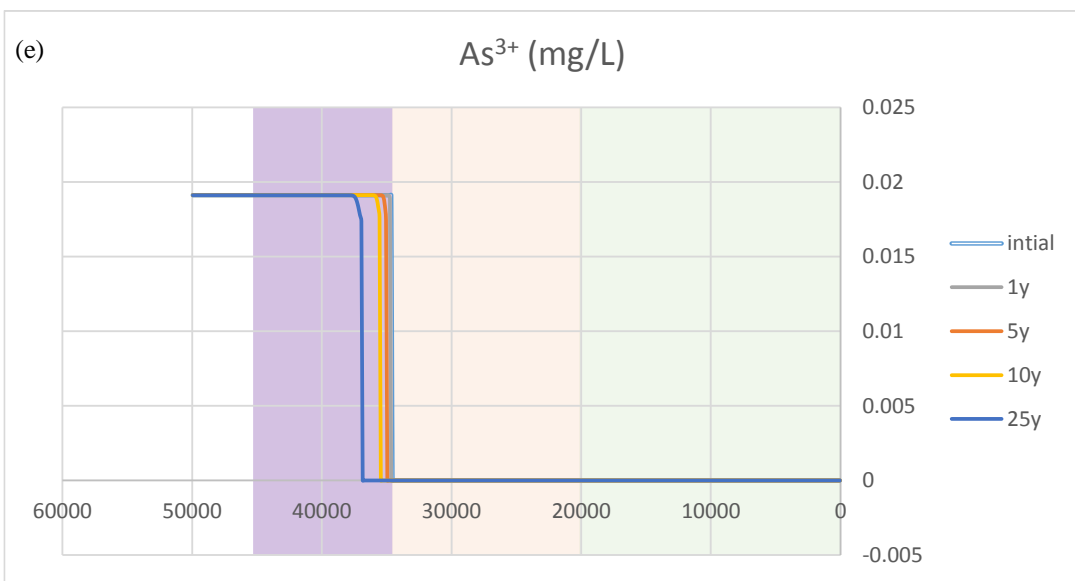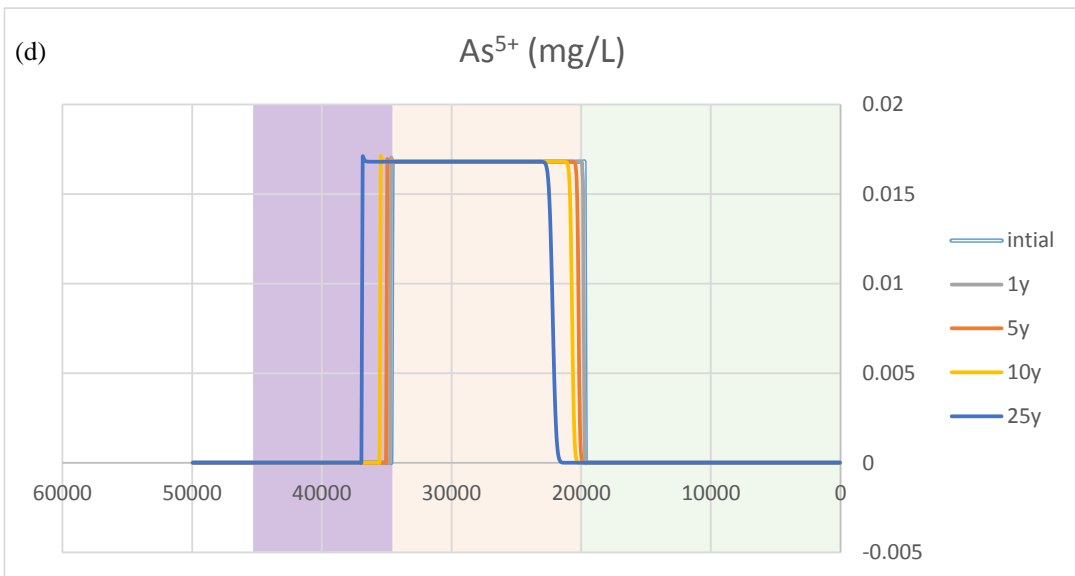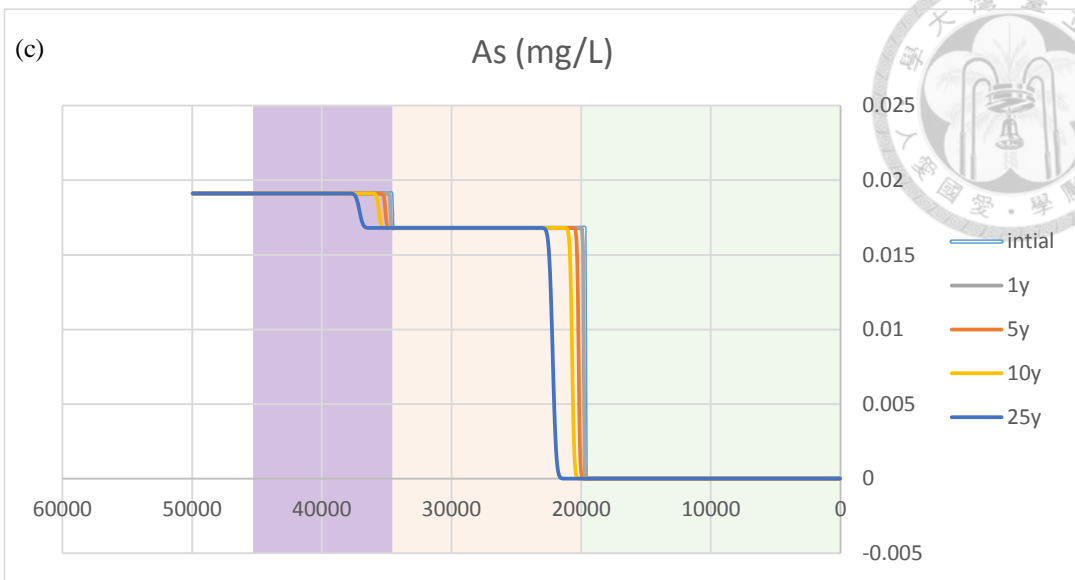
(c) As (mg/L)

(d) As^{5+} (mg/L)

(e) As^{3+} (mg/L)

Fig. 16 *(Cont'd)*
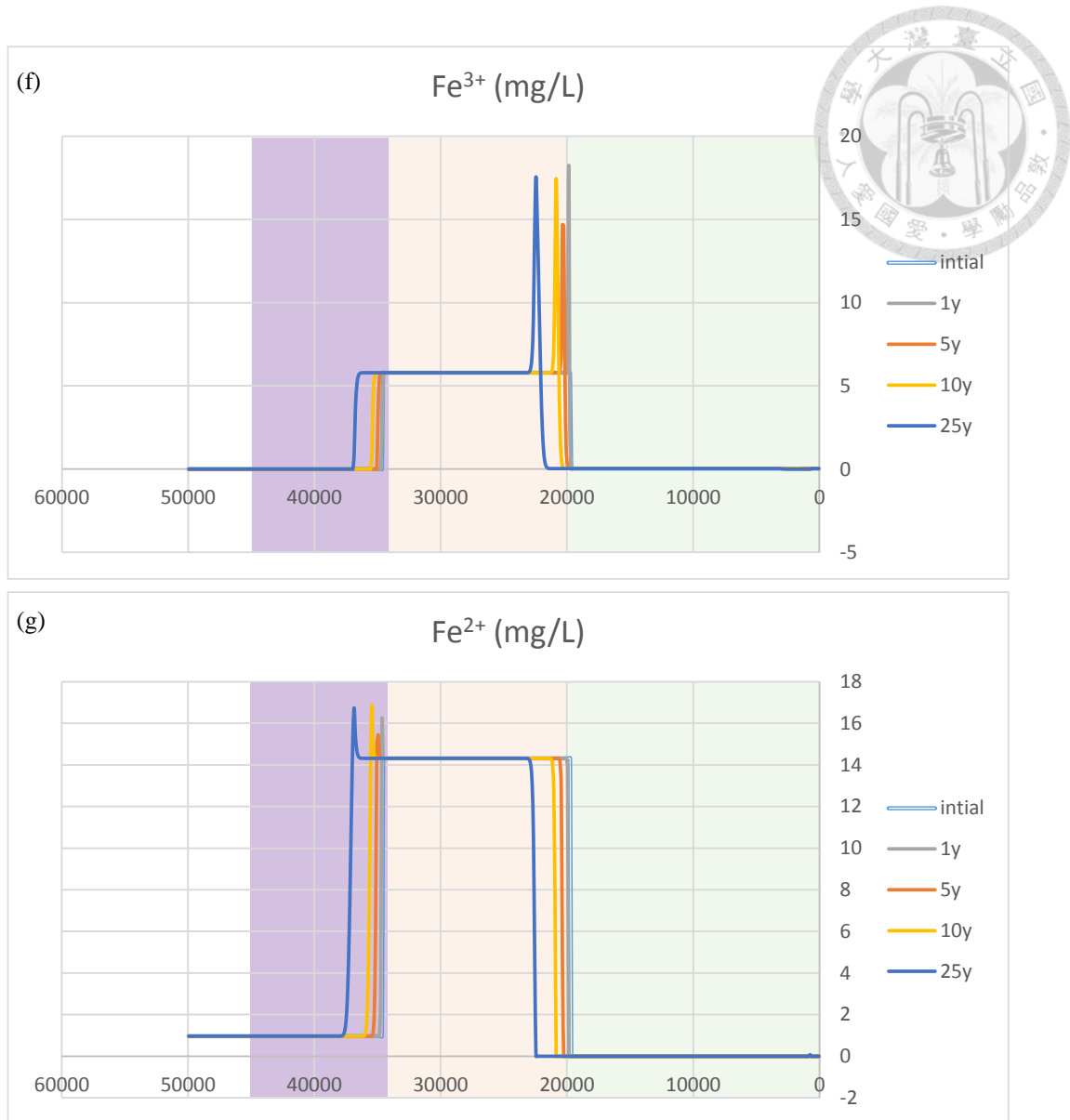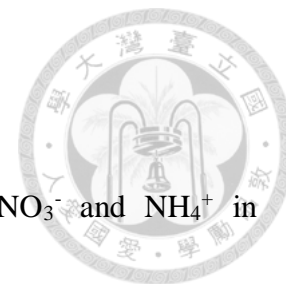
(f) Fe³⁺ (mg/L)

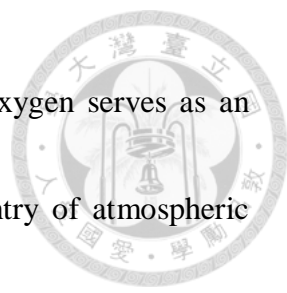(g) Fe²⁺ (mg/L)

Fig. 16 *(Cont'd)*

80

6. Conclusions

In this study, the sources causing high concentrations of NO_3^- and NH_4^+ in groundwater, the transformation within N-budget system of the sources, the contribution of nitrogen compounds to the release of As into groundwater, and the simulations of N transformation and transport in As-rich groundwater of Choushui river alluvial fan have been identified.

First, the results obtained for $\delta^{15}N_{NO3}$ and $\delta^{18}O_{NO3}$ suggest that NO_3^- denitrification by microorganisms may occur from the upstream region to the downstream region of the Choushui River. The NO_3^- concentrations decrease in the downstream direction.

The sources of NO_3^- in the proximal fan of the Choushui River alluvial fan may be ammonium fertilizers, soil ammonium, and manure and septic waste. Because the groundwater tends to be oxidative, NH_4^+ is converted to NO_3^- (nitrification) once the NH_4^+ sources infiltrate the groundwater, resulting in the enrichment of NO_3^-. However, there is no clear evidence for NO_3^- assimilation by living organisms or NO_3^- denitrification by microorganisms in the proximal fan.

The physicochemical characteristics and the relatively low value of $\delta^{18}O_{NO3}$ in the proximal fan of the Choushui River alluvial fan indicates the possibility of oxygen from

81

sources other than NO_3^- entering the groundwater. Atmospheric oxygen serves as an alternative to the oxygen in NO_3^- for microbial activities. The entry of atmospheric oxygen results from unconfined granular nature and overpumping of groundwater for agricultural activities.

The $\ln NO_3^-$ versus $\delta^{15}N_{NO3}$ plot for the mid-fan of the Choushui River alluvial fan suggests that NO_3^- assimilation and denitrification may occur in the groundwater. However, the ratio $\delta^{15}N/\delta^{18}O$ shows only mild denitrification, suggesting that NO_3^- assimilation by living organisms, rather than denitrification, is dominant and responsible for the depletion of NO_3^-. The environment of high concentrations of As, NH_4^+ and Fe, and the depletion of $\delta^{15}N_{NO3}$ suggest the occurrence of feammox process in the mid-fan, causing As to desorb from Fe oxyhydroxides and release to groundwater.

The NO_3^- sources in the mid-fan and the distal fan of the Choushui River alluvial fan appear to be nitrate fertilizers and marine nitrate. NO_3^- is assimilated and mineralized to NH_4^+ by heterorganic microbes or through DNRA in the reductive groundwater, leading to the enrichment of NH_4^+ in the groundwater. The $\ln NO_3^-$ versus $\delta^{15}N_{NO3}$ plot shows the possibility of NO_3^- assimilation and denitrification in the groundwater. The ratio $\delta^{15}N/\delta^{18}O$ in the distal fan indicates that NO_3^- denitrification is significant, and the

82

enrichment of both $^{15}N_{NO3}$ and $^{18}O_{NO3}$ support this indication. In other words, assimilation, mineralization, DNRA, and denitrification should occur simultaneously in the distal fan of the Choushui River alluvial fan, resulting in the depletion of NO_3^- and enrichment of NH_4^+ in the groundwater.

High NO_3^- concentrations in the groundwater of the proximal fan result in an oxidative environment, which is not favorable for the reductive dissolution of As-containing Fe oxyhydroxides. By contrast, feammox in the mid-fan and denitrification in the distal fan may lead to the reductive dissolution of As-containing Fe oxyhydroxides, resulting in the release of As into the groundwater; because of the reductive environment, NH_4^+ and As are present in considerable amounts.
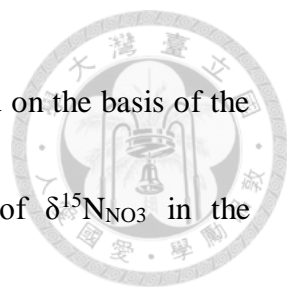
Furthermore, the PHREEQC simulation suggested that 92.31% of NH_4^+ in the proximal fan, 69.70% of NH_4^+ in the mid-fan, and 21.17% of NH_4^+ in the distal fan simulatively oxidized to NO_3^- through nitrification and/or feammox. These data clearly show that the nitrification and/or Feammox mostly occur in the proximal fan and mid-fan, whereas they slightly occur in the distal fan. The reaction of nitrification leads to the consequence of groundwater being abundant in NO_3^- and being depleted in NH_4^+. The mean concentrations of NO_3^- and NH_4^+ in the proximal fan are 23.62 mg/L and 0.17 mg/L,

respectively, evidently supporting the occurrence of NH_4^+ nitrification. Also, the proximal fan was assessed on the basis of local DO and ORP values to be in an oxidative state, initiatively urging the occurrence of nitrification.
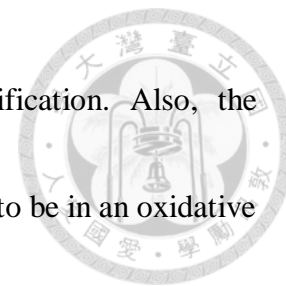
32.93% of NO_3^- in the mid-fan and 61.13% of NO_3^- in the distal fan simulatively reduced to N_2 or NH_4^+ through denitrification and/or DNRA. The spatial concentration distribution of NO_3^- from the proximal fan to the distal fan indicates the gradual occurrence of NO_3^- denitrification and/or DNRA from upstream to downstream of the Choushui River alluvial fan. Also, the mid-fan and the distal fan were assessed on the basis of the local DO and ORP values to be in relatively more reductive conditions, driving the occurrence of denitrification and/or DNRA. Moreover, the concentration of NH_4^+ in the distal fan indicates that in addition to denitrification, DNRA might be the dominant process of N cycling in the distal fan.

In the proximal fan, As^{3+} decreased by 1.32E−4 mg/L, and this valence transformation of As species and As concentration difference seem comprehensible. In the mid-fan and the distal fan, the reductive state was observed base on the DO and ORP data of the groundwater, and the circumstance of reduction from As^{5+} to As^{3+} was obvious, reaching 6.62E−3 mg/L and 6.40E−3 mg/L, respectively.

84

The discrepancy of $\delta^{15}N$ in NO_3^- in groundwater was simulated on the basis of the influence of the reaction of NO_3^- denitrification. The values of $\delta^{15}N_{NO3}$ in the groundwater of the mid-fan and the distal fan increased by +2.11% and +5.79%, respectively. The $\delta^{15}N$ value of the residual NO_3^- increases with a decrease in the NO_3^- concentration during denitrification. Further, the reductive environment further enhances the reductive dissolution of As-bearing Fe oxyhydroxides and the desorption of adsorbed As, resulting in the release of As into groundwater.

The 1-D transport simulation result suggested that NO_3^- assimilation occur from the mid-fan of the Choushui River Alluvial Fan to the distal fan, whereas NH_4^+ nitrification is observed at the beginning of the proximal fan. The initial and twenty-five years of NO_3^- and NH_4^+ transport have little shift backward but are insignificant.

The total amount of As increased along the upstream to the downstream of the Choushui River. The concentration of As^{5+} increased at the beginning of the mid-fan, which may be caused by the reductive dissolution of As-bearing Fe oxyhydroxides and the desorption of adsorbed As. The concentration of As^{3+} increased obviously at the beginning of the distal fan, which may be related to the transformation of As^{5+} to As^{3+} in the reductive environment, and the continuous desorption of As from Fe oxyhydroxides

85

simultaneously.

Both the concentrations of Fe^{3+} and Fe^{2+} increased at the end of proximal, causing by the reductive dissolution of Fe oxyhydroxides. The transformation of Fe^{3+} to Fe^{2+} occurred soon when the groundwater reached the mid-fan, resulting in depletion of Fe^{3+} and increase in Fe^{2+} in groundwater. The increase in Fe^{2+} is not only related to the reductive environment, but also attributed to the reaction of feammox, which Fe oxyhydroxides react with NH_4^+ and produce Fe^{2+} in the groundwater.

86

References

Agricultural Engineering Research Center. Analysis and evaluation of the groundwater quality survey in Taiwan, 2010; 2012. Taiwan Water Resource Bureau. Taipei.

Akai, J., Izumi, K., Fukuhara, H., Masuda, H., Nakano, S., Yoshimura, T., Ohfuji, H., Anawar, H.M., Akai, K., 2004. Mineralogical and geomicrobiological investigations on groundwater arsenic enrichment in Bangladesh. Applied Geochemistry. 19(2), 215-230.

Amberger, A., Schmidt, H.L., 1987. Natürliche isotopengehalte von nitrat als indikatoren für dessen Herkunft. Geochimica et Cosmochimica Acta. 51(10), 2699-2705.

Anawar, H.M., Tareq, S.M., Ahmed, G., 2013. Is organic matter a source or redox driver or both for arsenic release in groundwater? Physics and Chemistry of the Earth. 58-60, 49-56.

Andersson, K.K., Hooper, A.B., 1983. O_2 and H_2O are each the source of one O in NO_2^- produced from NH_3 by Nitrosomonus: ^{15}N-NMR evidence. FEBS Letters. 164(2), 236-240.

Andersson P, Torssander P, Ingri J. Sulphur isotope ratios in sulphate and oxygen isotopes in

water from a small watershed in central Sweden. Hydrobiologia 1992;235/236:205–17.

Aravena, R., Robertson, W.D., 1998. Use of multiple isotope tracers to evaluate denitrification in ground water: Study of nitrate from a large-flux septic system plume. Ground Water. 36(6), 975-982.

Brenot , A., Carignan, J., France-Lanord, C., Benoìt, M., 2007. Geological and land use control on $d^{34}S$ and $d^{18}O$ of river dissolved sulfate: the Moselle river basin, France. Chem. Geol. 244, 25-41.

Central Geological Survey. Project of groundwater monitoring network in Taiwan during first stage-research report of Chou-Shui River alluvial fan, Taiwan. Taiwan Water Resource Bureau Taipei. 1999. (In Chinese)

Cifuentes, L.A., Fogel, M.L., Pennock, J.R., Sharp, J.H., 1989. Biogeochemical factors that influence the stable nitrogen isotope ratio of dissolved ammonium in the Delaware Estuary. Geochimica et Cosmochimica Acta. 53(10), 2713-2721.

Clark I, Fritz P. Groundwater quality. In: Stein J, Starkweather AW, editors. Environmental isotopes in hydrogeology. Boca Raton (NY): Lewis; 1997. p. 142–3.

Cook, P.G.E., Herczeg, A.L.E., 2000. Environmental Tracers in Subsurface Hydrology. Kendall C, Aravena R, editors: Springer Science+Business Media, LLC, New York.

88

261-297 p.

Deutsch, B., Mewes, M., Liskow, I., Voss, M., 2006. Quantification of diffuse nitrate

inputs into a small river system using stable isotopes of oxygen and nitrogen in

nitrate. Organic Geochemistry. 37(10), 1333-1342.

Farooq, S.H., Chandrasekharam, D., Berner, Z., Norra, S., Stüben, D., 2010. Influence

of traditional agricultural practices on mobilization of arsenic from sediments to

groundwater in Bengal delta. Water Research. 44, 5575-5588.

Fukada, T., Hiscock, K.M., Dennis, P.F., 2004. A dual-isotope approach to the nitrogen

hydrochemistry of an urban aquifer. Applied Geochemistry. 19(5), 709-719.

Fukada, T., Hiscock, K.M., Dennis, P.F., Grischek, T., 2003. A dual isotope approach to

identify denitrification in groundwater at a river-bank infiltration site. Water

Research. 37(13), 3070-3078.

Hartland A, Larsen JR, Andersen MS, Baalousha M, O'Carroll D. Association of

Arsenic and Phosphorus with Iron Nanoparticles between Streams and Aquifers:

Implications for Arsenic Mobility. Environmental Science & Technology.

2015;49:14101-9.

Harvey, C.F., Swartz, C.H., Badruzzaman, A.B., Keon-Blute, N., Yu, W., Ali, M.A., Jay,
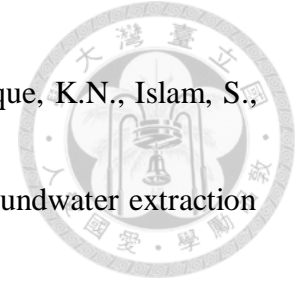
J., Beckie, R., Niedan, V., Brabander, D., Oates, P.M., Ashfaque, K.N., Islam, S., Hemond, H.F., Ahmed, M.F., 2002. Arsenic mobility and groundwater extraction in Bangladesh. Science. 298(5598), 1602-1606.

Hollocher, H.C., 1984. Source of the oxygen atoms of nitrate in the oxidation of nitrite by nitrobacter agilis and evidence against a P-O-N anhydride mechanism in oxidative phosphorylation. Archives of Biochemistry and Biophysics. 233(2), 721-727.

Hosono, T., Wang, C.H., Umezawa, Y., Nakano, T., Onodera, S., Nagata, T., Yoshimizu, C., Tayasu, I., Taniguchi, M., 2011. Multiple isotope (H, O, N, S and Sr) approach elucidates complex pollution causes in the shallow groundwaters of the Taipei urban area. J. Hydrol. 397, 23-36.

Hsu, C.H., Han, S.T., Kao, Y.H., Liu, C.W., 2010. Redox characteristics and zonation of arsenic-affected multi-layers aquifers in the Choushui River alluvial fan, Taiwan. Journal of Hydrology. 391(3-4), 351-66.

IAEA (International Atomic Energy Agency), 1983. Guidebook on Nuclear Techniques in Hydrology. Tech. Rep. Ser. 91, 439.

Ingraham, N.L. (1998). Isotopic variation in precipitation. Chpater3, In: Kendall C. and

McDonnell J.J. (eds), Isotope Tracers in Catchment Hydrology, Elsevier, Amsterdam, 87-118

Kao, Y.H., Liu, C.W., Wang, S.W., Lee, C.H., 2012. Estimating mountain block recharge to downstream alluvial aquifers from standard methods. Journal of Hydrology. 426-427, 93-102.

Kao, Y. H., Liu, C. W., Wang, S. W., Wang, P.L., Wang, C.H., Maji, S.K., 2011. Biogeochemical cycling of arsenic in coastal salinized aquifers: evidence from sulfur isotope study. Sci. Total Environ. 409, 4818-4830.

Karr, J.D., Showers, W.J., Gilliam, J.W., Andres, A.S., 2001. Tracing nitrate transport and environmental impact from intensive swine farming using delta nitrogen-15. Journal of Environmental Quality. 30(4), 1163-1175.

Kendall, C., 1998. Tracing nitrogen source and cycling in catchments. In: Kendall, C., McDonnell, J.J. (Eds.), Isotope Tracers in Catchment Hydrology. Elsevier Science B.V, The Netherlands, 519-576.

Kendall, C.E., McDonnell, J.J.E., 1998. Isotope Tracers in Catchment Hydrology. Caldwell EA, editors: Elsevier Science B.V., Amsterdam. 51-86 p.

Kinniburgh DG and Cooper DM. Predominance and mineral stability diagrams revisited.

Environmental Science & Technology. 2004;38:3641–8.

Kirk, M.F., Holm, T.R., Park, J., Jin, Q., Sanford, R.A., Fouke, B.W., Bethke, C.M., 2004. Bacterial sulfate reduction limits natural arsenic contamination in groundwater. Geology. 32(11), 953.

Kroopnick, P.M., Craig, H., 1972. Atmospheric oxygen: Isotopic composition and solubility fractionation. Science. 175(4017), 54-55.

Krouse, H.R., Mayer, B., 2000. Sulphur and oxygen isotopes in sulphate. In: Cook, P., Herczeg, A.L. (Eds.), Environmental Tracers in Subsurface Hydrology. Kluwer Academic Publishers, pp. 195–231.

Kumar, S., Nicholas, D.J.D., Williams, E.H., 1983. Definitive ^{15}N NMR evidence that water serves as a source of 'O' during nitrite oxidation by Nitrobacter agilis. FEBS Letters. 152(1), 71-74.

Kurosawa, K., Egashira, K., Masakazu, T., Jahiruddin, M., Abu Zofar, M., Moslehuddin, Zulfikar Rahman, M., 2008. Variation in arsenic concentration relative to ammonium nitrogen and oxidation reduction potential in surface and groundwater. Commun. Soil. Sci. Plan. 39, 1467-1475.

Liu, C.W., Lin, K.H., Kuo, Y.M., 2003. Application of factor analysis in the assessment

of groundwater quality in a blackfoot disease area in Taiwan. Science of The Total Environment. 313(1-3), 77-89.

Liu CW, Wang CJ, Kao YH. Assessing and simulating the major pathway and hydrogeochemical transport of arsenic in the Beitou–Guandu area, Taiwan. Environmental Geochemistry and Health. 2016;38:219-31.

Liu, C.W., Wang, S.W., Jang, C.S., Lin, K.H., 2006. Occurrence of arsenic in ground water in the Choushui river alluvial fan, Taiwan. J. Environ. Qual.35, 68-75.

Liu, K.K., 1984. Hydrogen and oxygen isotopic compositions of meteoric waters from the Tatun Shan area, northern Taiwan. Bull. Inst. Earth Sci. Acad. Sin. 4, 159-175.

Liu, C.W., Lin, K.H., Kuo, Y.M., 2003. Application of factor analysis in the assessment of groundwater quality in a blackfoot disease area in Taiwan. Sci. Total Environ. 313, 77-89.

Lu, K.L., Liu, C.W., Liao, V.H.C., Liao, C.M., 2016. Distinct function of metal-reducing bacteria from sediment and groundwater in controlling the arsenic mobilization in sedimentary aquifer. Journal of Bioremediation & Biodegradation. 07(01).

Lu, K.L., Liu, C.W., Wang, S.W., Jang, C.S., Lin, K.H., Liao, V.H.C., Laio, C.M., Chang, F.J., 2010. Primary sink and source of geogenic arsenic in sedimentary aquifers in the southern Choushui River alluvial fan, Taiwan. Applied Geochemistry. 25(5),

684-695.

Mapoma HWT, Xie X, Pi K, Liu Y, Zhu Y. Understanding arsenic mobilization using

reactive transport modeling of groundwater hydrochemistry in the Datong basin

study plot, China. Environmental Science Process & Impacts. 2016;18:371-85.

Mariotti, A., Landreau, A., Simon, B., 1988. ^{15}N isotope biogeochemistry and natural

denitrification process in groundwater: Application to the chalk aquifer of northern

France. Geochimica et Cosmochimica Acta. 52(7), 1869-1878.

Mayorga, P., Moyano, A., Anawar, H.M., García-Sánchez, A., 2013. Temporal variation

of arsenic and nitrate content in groundwater of the Duero River Basin (Spain).

Physics and Chemistry of the Earth, Parts A/B/C. 58-60, 22-7.

Mengis, M., Schif, S.L., Harris, M., English, M.C., Aravena, R., Elgood, R.J., Maclean,

A., 1999. Multiple geochemical and isotopic approaches for assessing ground water

NO_3^- elimination in a riparian zone. Ground Water. 37(3), 448-457.

Michener, R.H.E., Lajtha, K.E., 2007. Stable Isotopes in Ecology and Environmental

Science. Kendall C, Elliott EM, Wankel SD, editors: Blackwell Publishing,

Hoboken, New Jersey. 375-449 p.

Montoya, J.P., Korrigan, S.G., McCarthy, J.J., 1991. Rapid, storm-induced changes in

the natural abundance of ^{15}N in a planktonic ecosystem, Chesapeake Bay, USA.

Geochimica et Cosmochimica Acta. 55(12), 3627-3638.

Mukherjee, A., Sengupta, M.K., Hossain, M.A., Ahamed, S., Das, B., Nayak, B., Lodh, D.,

Rahman, M.M., Chakraborti, D., 2006. Arsenic contamination in groundwater: a global

perspective with emphasis on Asian scenario. J. Health Popul. Nutr. 24, 142-163.

Nickson, R.T., McArthur, J.M., Ravenscroft, P., Burgess, W.G., Ahmed, K.M., 2000.

Mechanism of arsenic release to groundwater, Bangladesh and West Bengal.

Applied Geochemistry. 15(4), 403-413.

Seiler RL, Stillings LL, Cuter N, Salonen L, Outola I. Biogeochemical factors affecting the

presence of 210Po in groundwater. Appl. Geochem 2011; 26:526–39.

Otero, N., Soler, A., Canals, À., 2008. Controls of d^{34}S and d^{18}O in dissolved sulphate: Learing

from a detailed survey in the Llobregat River (Spain). Appl. Geochem. 23, 1166-1185.

Panno, S.V., Hackley, K.C., Kelly, W.R., Hwang, H.H., 2006. Isotopic evidence of

nitrate sources and denitrification in the Mississippi River, Illinois. Journal of

Environmental Quality. 35(2), 495-504.

Parkhurst DL and Appelo CAJ. User's guide to PHREEQC (version 2)--A computer

program for speciation, batch-reaction, one-dimensional transport, and inverse

geochemical calculations: U.S. Geological Survey Water-Resources Investigations

Report. 1999. 99-4259, 312 p.

Pauwels, H., Foucher, J.C., Kloppmann, W., 2000. Denitrication and mixing in a schidt

aquifer: influence on water chemistry and isotopes. Chemical Geology. 168, 307-

324.

Peng, T.R., Fan, C. H., 2005. Sources and Transformations of NO_3^- in waters of Li-Shan

agriculture area. Soil and Environment 8, 43–58. (In Chinese)

Peng, T.R., Lin, H.J., Wang, C.H., Liu, T.S. and Kao, S.J., 2012. Pollution and variation of

stream nitrate in a protected high-mountain watershed of Central Taiwan: evidence from

nitrate concentration and nitrogen and oxygen isotope compositions. Environ. Monit.

Assess. 184, 4985-4998.

Peng, T. R., Wang, C.H., Lai, T.C., Ho F. S.K., 2007. Using hydrogen, oxygen, and tritium

isotopes to identify the hydrological factors contributing to landslides in a mountainous

area, central Taiwan, Environ. Geol. 52, 1617-1629.

Peng, T. R., Zhan, W. J., Lin, Y. U., & Liu, C. L., 2004. Evaluation of the origin and

transformation of nitrate in river water of Nantou area using the nitrogen isotope in NO_3^-.

Soil and Environment 7, 167–182. (In Chinese)

96
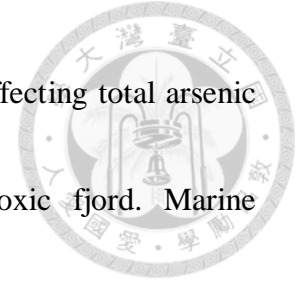
Peterson, M.L., Carpenter, R., 1983. Biogeochemical processes affecting total arsenic and arsenic species distributions in an intermittently anoxic fjord. Marine Chemistry. 12, 295-321.

Pierce, M.L., Moore, C.B., 1982. Adsorption of arsenite and arsenate on amorphous iron hydroxide. Water Research. 16, 1247-1253.

Pi, K.F., Wang, Y.X., Xie, X.J., Huang, S.B., Yu, Q., Yu, M., 2015. Geochemical effects of dissolved organic matter biodegradation on arsenic transport in groundwater systems. Journal of Geochemical Exploration. 149, 8-21.

Plant, J.A., Kinniburgh, D.G., Smedley, P.L., Fordyce, F.M., Klinck, B.A., 2005. Arsenic and Selenium. In: Lollar, B.S. (Ed.), Environmental Geochemistry, vol. 9. In: Holland, H.D., Turekian, K.K. (Eds.), Treatise on Geochemistry. Elsevier- Pergamon, Oxford, 17-66.

Polizzotto, M.L., Kocar, B.D., Benner, S.G., Sampson, M., Fendorf, S., 2008. Near-surface wetland sediments as a source of arsenic release to ground water in Asia. Nature 454, 505-509.

Postma D, Larsen F, Hue NTM, Duc MT, Viet PH, Nhan PQ, et al. Arsenic in groundwater of the Red River floodplain, Vietnam: Controlling geochemical processes and reactive transport modeling. Geochimica et Cosmochimica Acta. 2007;71:5054-71.
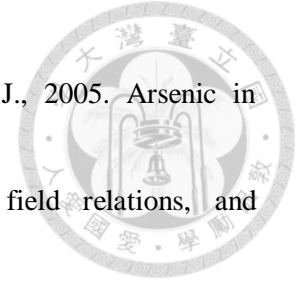
Ravenscroft, P., Burgess, W.G., Ahmed, K.M., Burren, M., Perrin, J., 2005. Arsenic in groundwater of the Bengal basin, Bangladesh: distribution, field relations, and hydrogeologic setting. Hydrogeol. J. 13, 727-751.

Robinson, B.W., Bottrell, S.H., 1997. Discrimination of sulfur source in pristine and polluted New Zealand river catchments using stable isotopes. Appl. Geochem. 12, 305-319.

Seiler, R.L., Stillings, L.L., Cuter, N., Salonen, L., Outola, I., 2011. Biogeochemical factors affecting the presence of 210Po in groundwater. Appl. Geochem. 26, 526-539.

Seiler, R.L., 2005. Combined use of ^{15}N and ^{18}O of nitrate and ^{11}B to evaluate nitrate contamination in groundwater. Applied Geochemistry. 20(9), 1626-1636.

Sengupta S, Sracek O, Jean JS, Lu HY, Wang CH, Palcsu L, et al. Spatial variation of groundwater arsenic distribution in the Chianan Plain, SW Taiwan: Role of local hydrogeological factors and geothermal sources. Journal of Hydrology. 2014;518:393-409.

Sharp, Z., 2007. Principles of Stable Isotope Geochemistry: Pearson/Prentice Hall, Upper Saddle River, New Jersey. 64-102.

Sigman, D.D. Casciotti, K.L. Andreani, M. Barford,C. Galanter, M. Bohlke, J. K. A Bacterial Method for the Nitrogen Isotopic Analysis of Nitrate in Seawater and Freshwater. Anal. Chem. 2001, 73, 4145-4153.

Smedley, P.L., Kinniburgh, D.G., 2002. A review of the source, behavior and distribution

of arsenic in natural waters. Applied Geochemistry. 17(5), 517-568.

Stüben, D., Berner, Z., Chandrasekharam, D., Karmakar, J., 2003. Arsenic enrichment in

groundwater of West Bengal, India: geochemical evidence for mobilization of As under

reducing conditions. Appl. Geochem. 18, 1417-1434.

Torssander, P., Morth, C.M., Kumpulainen, R., 2006. Chemistry and sulfur isotope investigation

of industrial wastewater contamination into groundwater aquifers, Pitea County, N. Sweden.

J. Geochem. Explor. 88, 64-67.

Swartz, C.H., Blute, N.K., Badruzzman, B., Ali, A., Brabander, D., Jay, J., Besancon, J.,

Islam, S., Hemond, H.F., Harvey, C.F., 2004. Mobility of arsenic in a Bangladesh

aquifer: Inferences from geochemical profiles, leaching data, and mineralogical

characterization. Geochimica et Cosmochimica Acta. 68(22), 4539-4557.

Umezawa, Y., Hosono, T., Onodera, S.I., Siringan, F., Buapeng, S., Delinom, R.,

Yoshimizug, C., Tayasuh, I., Nagatai, T., Taniguchia, M., 2009. Erratum to

"Sources of nitrate and ammonium contamination in groundwater under

developing Asian megacities". Science of the Total Environment.407(9), 3219-

3231.

Tekin, E., 2012. Anaerobic ammonium oxidation in groundwater contaminated by fertilizers. Master's thesis, University of Ottawa, Ottawa, Canada.

Thurman EM. Organic Geochemistry of Natural Waters. M. Nijhoff and W. Junk Publishers: Dordrecht, the Netherlands, 1985.

Vitòria, L., Otero, N., Soler, A., Canals, À., 2004. Fertilizer characterization: isotopic data (N, S, O, C, and Sr). Environ. Sci. Technol. 38, 3254-3262.

Wang, C.H., Kuo, C.H., Peng, T.R., Chen, W.F., Chiang, C.J., Liu, W.C., Hung, J.J., 2000. Stable isotope characteristics of Taiwan groundwaters. The symposium on Taiwan quaternary & workshop of the Asia paleoenvironmental change project. p. 3

Wang, C.H., Peng T.R., 2001. Hydrogen and oxygen isotopic compositions of Taipei precipitation: 1990–1998. Western Pacific Earth Sci. 1(4), 429-442.

Wang, S.W., Liu, C.W., Jang, C.S., 2007. Factors responsible for high arsenic concentrations in two groundwater catchments in Taiwan. Appl. Geochem. 22, 460-467.

Weng TN, Liu CW, Kao YH, Hsiao SSY. Isotopic evidence of nitrogen sources and nitrogen transformation in arsenic-contaminated groundwater. Science of the Total Environment. 2017;578:167-85

Xiong, F., Gan, Y., Duan, Y., 2015. Analysis of relationship between nitrogen and the

migration and enrichment of arsenic in groundwater in the Jianghan Plain. Safety and Environmental Engineering. 22(2), 39-48.

Yang, W.H., Weber, K.A., Silver, W.L., 2012. Nitrogen loss from soil through anaerobic ammonium oxidation coupled to iron reduction. Nature Geoscience. 5(8), 538-541.

Zhang, X., Sigman, D.M., Morel, F.M.M., Kraepiel, A.M.L., 2014. Nitrogen isotope fractionation by alternative nitrogenases and past ocean anoxia. Proceedings of the National Academy of Sciences of the United States of America. 111(13), 4782-4787.